IN THIS ISSUE

IMAGE: OBSERVATORY WITH STAR TRAILS ON MOUNTAINS FOR CLEAR SKY

London Journals Press

www.journalspress.com

LONDON JOURNAL OF ENGINEERING RESEARCH

Print ISSN: 2631-8474
Online ISSN: 2631-8482
DOI: 10.17472/LJER

Volume 22 | Issue 3 | Compilation 1.0

COMPILED IN UNITED KINGDOM

ENGLISH

London Journal of Engineering Research

Volume 22 | Issue 3 | Compilation 1.0

PUBLISHER

London Journals Press
1210th, Waterside Dr, Opposite Arlington Building, Theale, Reading
Phone:+444 0118 965 4033 Pin: RG7-4TY United Kingdom

SUBSCRIPTION

Frequency: Quarterly

Print subscription
$280USD for 1 year
$500USD for 2 year
(color copies including taxes and international shipping with TSA approved)

Find more details at https://journalspress.com/journals/subscription

ENVIRONMENT

London Journals Press is intended about protecting the environment. This journal is printed using led free environmental friendly ink and acid-free papers that are 100% recyclable.

London Journals Press Headquaters

1210th, Waterside Dr,
Opposite Arlington
Building, Theale, Reading
Phone:+444 0118 965 4033
Pin: RG7-4TY
United Kingdom

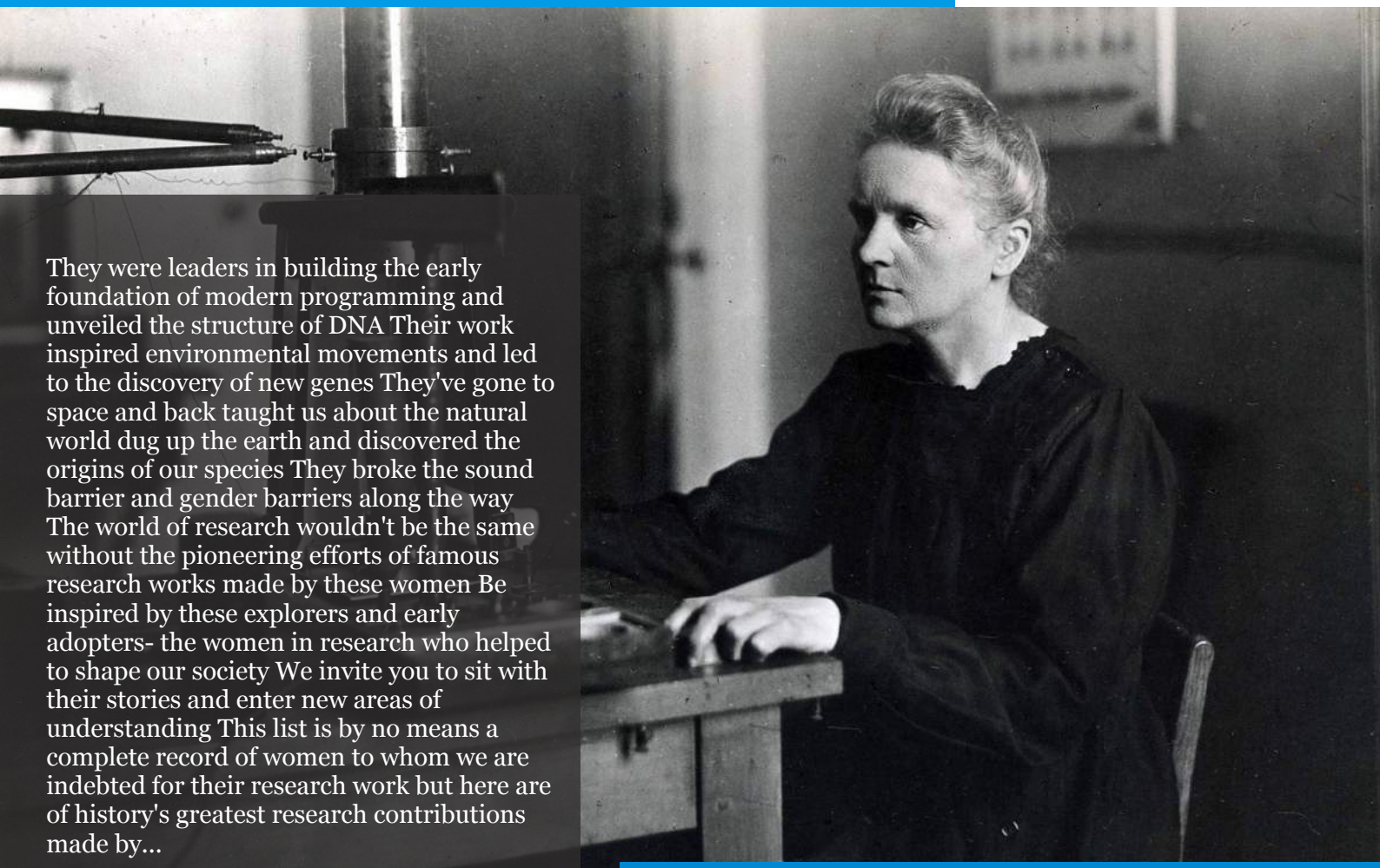

They were leaders in building the early foundation of modern programming and unveiled the structure of DNA Their work inspired environmental movements and led to the discovery of new genes They've gone to space and back taught us about the natural world dug up the earth and discovered the origins of our species They broke the sound barrier and gender barriers along the way The world of research wouldn't be the same without the pioneering efforts of famous research works made by these women Be inspired by these explorers and early adopters- the women in research who helped to shape our society We invite you to sit with their stories and enter new areas of understanding This list is by no means a complete record of women to whom we are indebted for their research work but here are of history's greatest research contributions made by...

Read complete here:
https://goo.gl/1vQ3lS

Women In Research

Computing in the cloud!

Cloud Computing is computing as a Service and not just as a Product Under Cloud Computing...

Read complete here:
https://goo.gl/VvHC72

Writing great research...

Prepare yourself before you start Before you start writing your paper or you start reading other...

Read complete here:
https://goo.gl/np73jP

Journal Content
In this Issue

London Journals Press

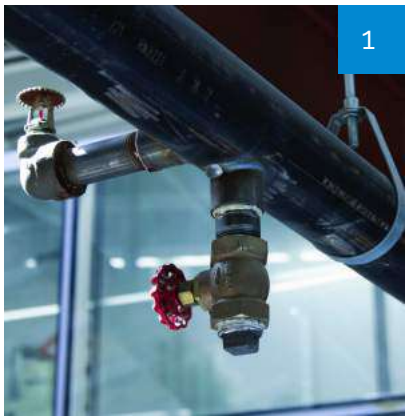

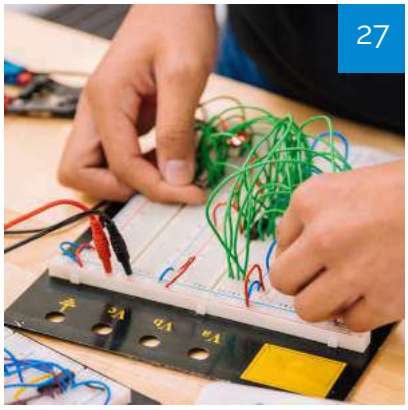

Editorial Board

Curated board members

Study on Self-locking Forward and Reverse Drill Pipe in Rod

Yi-Kang Tang & Chun-Dong Xu

Nanjing University of Science and Technology

ABSTRACT

Most of the drill pipes used by coal mine drilling rigs are connected by conical thread joints, which have good alignment and meet the working condition of one-way rotation and torsion, but can not rotate in reverse. A new type of self locking forward and reverse drill pipe structure in the rod was studied to realize the mechanical self-locking of thread pair connection and the automatic release of drill pipe machinery. From the back to the previous releases, the drill pipe connection has good rigidity, large bearing torque and good stability, which can meet the requirements of automatic addition of drill pipe.

Keywords: self-locking; forward and reverse drill pipe; sticking drill; holding drill.

Classification: DDC Code: 785 LCC Code: M5

Language: English

London Journals Press

LJP Copyright ID: 392941
Print ISSN: 2631-8474
Online ISSN: 2631-8482

London Journal of Engineering Research

Volume 22 | Issue 3 | Compilation 1.0

Study on Self-locking Forward and Reverse Drill Pipe in Rod

Yi-Kang Tang[α] & Chun-Dong Xu[σ]

ABSTRACT

Most of the drill pipes used by coal mine drilling rigs are connected by conical thread joints, which have good alignment and meet the working condition of one-way rotation and torsion, but can not rotate in reverse. A new type of self locking forward and reverse drill pipe structure in the rod was studied to realize the mechanical self-locking of thread pair connection and the automatic release of drill pipe machinery. From the back to the previous releases, the drill pipe connection has good rigidity, large bearing torque and good stability, which can meet the requirements of automatic addition of drill pipe.

Keywords: self-locking; forward and reverse drill pipe; sticking drill; holding drill.

Author α σ: School of Mechanical Engineering, Nanjing University of Science and Technology, Nanjing City, Jiangsu Province, China, 210094.

I. INTRODUCTION

Most of the drill pipes used in the drilling of coal mine drilling rigs are conical and threaded joints, which have good neutrality and can meet the one-way twisting condition, but also have the defect of not being able to rotate in the opposite direction. In the actual process of underground drilling in coal mines, the phenomenon of hole collapse is very likely to occur due to the influence of complex strata, which will lead to sticking and drilling accidents, which need to be reversed to assist in solving. At this time, there is no problem with the reversal of the power head of the drilling rig. The conventional ordinary drill pipes in the hole are threadedly connected and cannot be reversed. Therefore, a drill pipe capable of forward and reverse rotation is required to solve the problem that the thread does not loosen during reverse rotation.

At present, the forward and reverse drill pipes are mainly plug-in type to transmit the forward and reverse torque, and the axial positioning connection is performed with key pins or screws to transmit the axial load. The main problem is that the drill pipe needs to be manually unlocked For disassembly, the torque application range is small, the gap at the joint is large, the deflection of the drill pipe is large, and the mechanical automatic disassembly cannot be realized.

II. IN-ROD SELF-LOCKING FORWARD AND REVERSE DRILL ROD STRUCTURE

The self-locking forward and reverse drill pipe in the rod consists of a core tube, an outer tube, a limit pin, a spring limit ring, and a spring. The overall structure is shown in Figure 1

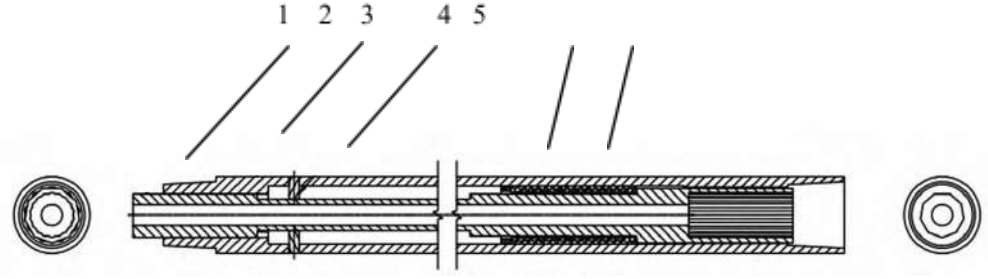

Figure 1: Schematic diagram of the structure of the self-locking forward and reverse drill pipe in the rod
1. Core tube 2. Outer tube 3. Limit pin 4. Spring limit ring 5. Spring

The new structure of the outer pipe is shown in Figure 2. The internal structure of the male joint is designed as an inner polygon. The shape is the same as that of the ordinary drill pipe. It is made of friction welding of the male joint, the female joint and the steel pipe to realize the extension and torque of the drill pipe. The front and rear ends are respectively provided with connecting threads and tooth-shaped grooves matched with the core pipe, and the pipe body and the joints at both ends are friction welded.

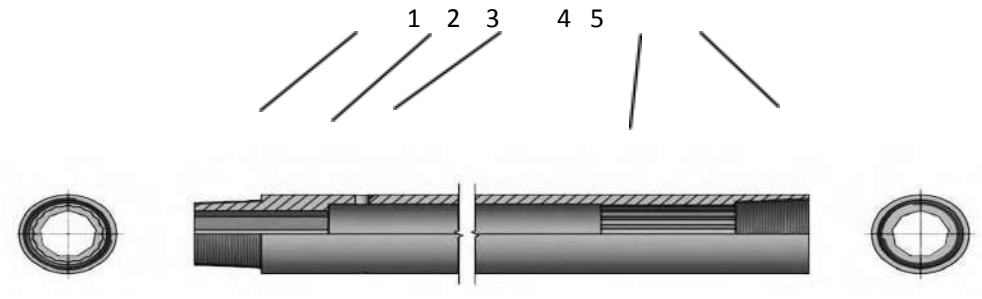

Figure 2: Schematic diagram of the outer tube structure

1. Male thread 2. Male internal tenon 3. Limit pin hole 4. Female internal tenon 5. Female thread

The male thread and the female thread complete the length of the drill pipe and carry the drilling torque; the inner tenon of the male head and the male tenon of the core pipe are clearance fit to carry the anti-rotation torque, and the male tenon of the core pipe can slide along the axial direction; the limit pin hole is determined The position of the limit pin bears the thrust of the spring; the limit pin moves to a suitable position after the core tube is loaded into the outer tube, and the insertion limit pin is welded firmly to limit the core tube from slipping out of the outer tube (drill pipe); the inner tenon of the female head and the core The pipe transition tenon is matched and can move along the axis, and the core tube female tenon transmits torque to the drill pipe through the transition tenon to realize the interlocking of the drill pipe.

The structure of the core tube is shown in Figure 3. The outer shape of one end is an outer polygon, which cooperates with the inner polygon of the outer tube male joint to transmit the torque load; Matching, realizes that the taper thread pair of the male and female joints of adjacent drill pipes is tightened to form a self-locking taper thread pair in the matching rod. The taper thread pair does not disengage when reversed (the drill pipe can be reversed), and there is a water supply through hole in the center.

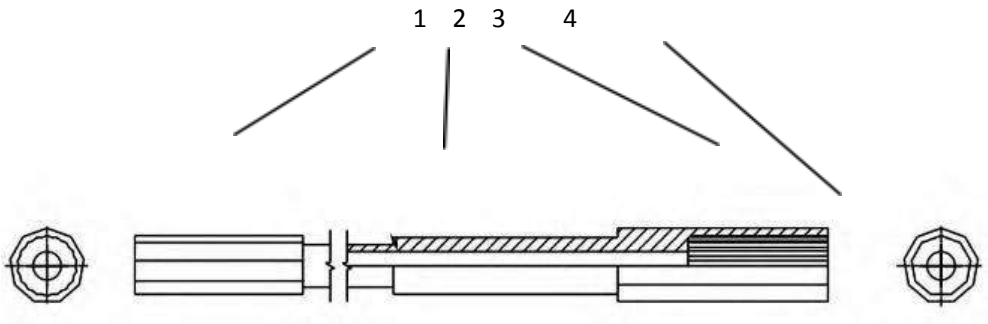

Figure 3: Schematic diagram of the core tube structure

1. Self-locking male tenon 2. Water hole 3. Self-locking female tenon 4. Transition tenon

The self-locking male tenon and the self-locking female tenon are composed of regular polygons, which are located at the male joint end of the drill pipe, and are toothed with the male joint to carry the anti-rotation torque. When self-locking, the self-locking female tenon is inserted; the water passage is the flushing water channel; The transition tenon is located at the end of the core tube and is a regular polygon, which transmits the torque of the male tenon to the female end of the drill pipe.

When the taper thread of the latter drill pipe joint is tightened through the limit pin, the spring limit ring and the spring between the outer tube and the core tube, the inner core tube is pushed to compress the spring, and the outer polygonal structure at the front end of the core tube extends into the previous one. The inner polygonal structure of the drill pipe core tube is matched to realize the self-locking and reversing functions of the drill pipe thread pair. After each drill pipe is connected, the last end is connected with the drilling water supply water braid thread pair to realize the self-locking of the last drill pipe. The first drill pipe male joint and the inner polygon at the root of the taper thread of the drill bit realize the self-locking of the first taper thread pair.

In the process of drilling and drilling, all drill pipes rely on the inner and outer polygonal structures of adjacent drill pipes to realize mechanical self-locking. Any forward and reverse construction operations will not cause the loosening of the thread pairs between the drill pipes. The outer polygonal structure of the core pipe not only cooperates with the polygonal structure in the male joint of its own outer pipe, but also cooperates with the polygonal structure in the inner core pipe of the latter drill pipe to bear the drilling torque. Since it is a multilateral load bearing, it can bear a large torque.

After the drilling construction is completed, when disassembling the drill pipe, it can only start from the last thread pair. After removing the tail water braid, the inner core pipe of the last drill pipe moves the core pipe backward under the elastic force of the spring, releasing the thread. The first thread pair (male joint thread pair) in front of the drill pipe unlocks the self-locking of one drill pipe, removes one drill pipe from the back to the front in turn, releases the self-locking of the adjacent previous drill pipe, and gradually unlocks the drill pipes one by one Taper thread pair.

The spring limit ring defines the position of the spring and realizes the compression of the spring. The spring realizes the reset of the core tube and completes the unlocking of the drill pipe.

III. THE WORKING PRINCIPLE OF THE SELF-LOCKING FORWARD AND REVERSE DRILL PIPE IN THE ROD

In-rod self-locking forward and reverse drill pipe is a drill pipe mechanism that uses the conditional interlocking principle between adjacent drill pipe joint threads to realize the forward and reverse interlocking of drill pipes., use the self-locking core pipe of the middle drill pipe to insert the self-locking core pipe of the last drill pipe during the screwing process of the last drill pipe and insert the core pipe of the most front drill pipe to realize the interlocking of the joints of the first two pipes, remove the last drill pipe, and the intermediate core pipe is under the spring force Under the action of the automatic reset, realize the unlocking of the first two drill pipe joints, so as to achieve the reverse self-locking function of the drill pipe.

The working principle of the self-locking forward and reverse drill pipe in the rod is shown in Figure 4.

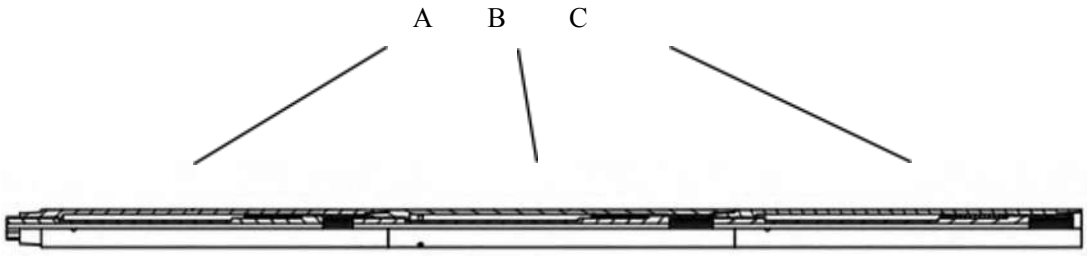

Figure 4: Working principle diagram of self-locking forward and reverse drill pipe in the rod

Three adjacent drill rods are connected in sequence, drill rods A and B are connected, and the male thread of drill rod B is screwed into the female thread of drill rod A to realize the connection of drill rods. At this time, there is no interlock between drill rods A and B; C drill pipe add-on, C drill pipe male thread is screwed into B drill pipe female thread; C drill pipe male joint pushes the core pipe forward, core pipe self-locking male tenon is inserted into A drill pipe self-locking female tenon, realizes A, B Interlock of drill pipe.

When the drill pipe is disassembled, the drill pipe can only be unlocked sequentially from the back to the front, and the drill pipe can be disassembled in sequence. Unscrew the male thread of the drill pipe C; the core pipe of the drill pipe B moves out of the self-locking female tenon of the core pipe of the A drill pipe under the action of the spring, so as to unlock the drill pipes A and B; Unlocking of the previous drill pipe.

III. CONCLUSION

The traditional forward and reverse drill pipe relies on the fluid pressure of the medium in the hole to push the piston, and the piston pushes the limiter to move radially and insert it into the thread groove, thereby limiting the thread rotation. The pressure in the hole and the tightness of the piston in the hole affect the solution of the drill pipe. Card success rate. This paper studies a new type of self-locking forward and reverse drill pipe in the rod, and introduces its structure and working principle in detail.

Through the mechanical structure, the self-locking of the drill pipe thread pair is realized, which has high reliability, large bearing torque and load, and good stability. The problem of connecting rods of traditional drill pipes is avoided, and a new and reliable design idea of forward and reverse drill pipes is provided.

REFERENCES

1. Pu Lianggui. Mechanical Design [M]. Beijing: Higher Education Press, 1991.
2. Cheng Daxian. Mechanical Design Manual [M]. Beijing: Chemical Industry Press, 2013.

Artificial Intelligence Applied in the Detection and Fault Localization in Dynamic Systems

Igor Feliciani Merizio, Fábio Roberto Chavarette & Estevão Fuzaro de Almeida

São Paulo State University

ABSTRACT

A methodology using artificial intelligence for diagnosing structures and predicting failures in mechanical systems is presented. An Artificial Immune System (AIS) able to identify and locate faults with good predictability was developed, having its operation based on the Negative Selection Algorithm (NSA). The Negative Selection Algorithm is divided into two steps: Censor phase and Monitoring. In the first step, the algorithm can learn about the normal operation of the system and created a baseline. In the second step, the algorithm evaluates the system data and becomes able to identify patterns different from what has been learned, in other words, a possible failure. The algorithm developed was optimized with the Clonal Selection Algorithm (ClonalG), aiming at fewer data in training.

Keywords: structural health monitoring; artificial immune system; negative selection algorithm; clonalg; fault detection.

Classification: DDC Code: 006.3 LCC Code: Q335

Language: English

London Journals Press

LJP Copyright ID: 392942
Print ISSN: 2631-8474
Online ISSN: 2631-8482

London Journal of Engineering Research

Volume 22 | Issue 3 | Compilation 1.0

Artificial Intelligence Applied in the Detection and Fault Localization in Dynamic Systems

Igor Feliciani Merizio[α], Fábio Roberto Chavarette[σ] & Estevão Fuzaro de Almeida[ρ]

ABSTRACT

A methodology using artificial intelligence for diagnosing structures and predicting failures in mechanical systems is presented. An Artificial Immune System (AIS) able to identify and locate faults with good predictability was developed, having its op eration based on the Negative Selection Algorithm (NSA). The Negative Selection Algorithm is divided into two steps: Censor phase and Monitoring. In the first step, the algorithm can learn about the normal operation of the system and created a baseline. In the second step, the algorithm evaluates the system data and becomes able to identify patterns different from what has been learned, in other words, a possible failure. The algorithm developed was optimized with the Clonal Selection Algorithm (ClonalG), aiming at fewer data in training. The results obtained suggest that the AIS can learn about the normal system operation using 5% of the available data, being able to diagnose with an excellent safety margin the predictability of a failure and inform where it is located. With the optimization by ClonalG the need for training data is reduced by 50% and the deviation adopted by 70%, without jeop- ardizing the algorithm hit rate. Thus, the algorithm optimized by ClonalG proved to be an excellent tool in the prevention of failures and accidents, presenting general hit rates above 99.90%. The differentials of this work are the high hit rate presented by the AIS, which performs few misclassifications, and the fact that modeling is not necessary. The system is able to learn by itself about the behavior of the data.

Keywords: structural health monitoring; artificial immune system; negative selection algorithm; clonalg; fault detection.

Author α ρ: Department of Mechanical Engineering, São Paulo State University, Av. Brasil, 56, Downtown, Ilha Solteira, SP, Brazil.

σ: Department of Engineering, Physics and Mathematics, São Paulo State University, R. Prof. Francisco Degni, 55, Quitandinha, Araraquara, SP, Brazil.

I. INTRODUCTION

The current and important line of research called Structural Health Monitoring (SHM) aims to detect failures in the initial states, intervening in the propagation of the failure and consequently preventing disasters and accidents occur causing the stopping or damaging the structure. As highlighted in Hall (1999), an SHM must have the following requirements:

- data acquisition and processing;
- validation and analysis of signals;
- identification and characterization of failures;
- interpretation of adverse changes in a structure;
- assist decision making.

In the literature, many works addressing the monitoring and diagnosis of failures have been identified and some are presented with a focus on the application of computational intelligence techniques such as: artificial neural networks Pandey and Barai (1995); Zheng, Wang, and Liu (2004), genetics algorithms Chen et al. (2007); Merizio, Chavarette, Moro, and Outa (2020), neural networks and wavelet transform Santi- ago et al. (2004), an electrical impedance technique combined with artificial neural networks Lopes Jr, Turra, Mu¨ller, Brunzel, and Inman (2001), electrical impedance technique with genetic algorithms Tebaldi (2004), piezoelectric sensors and actuators in artificial neural networks Giurgiutiu and Cuc (2005), PZTs Flynn and Todd (2010), Fuzzy logic Chandrashekhar and Ganguli (2009), electromechanical impedance technique Pita, Turra, and Vieira Filho (2013), wavelet transform Abreu, Chavarette, Villarreal, Duarte, and Lima (2014); Qiu, Lee, Lin, and Yu (2006) , artificial immunological algorithms F. Lima,

Lotufo, and Minussi (2013), intelligent hybrid algorithms Parra dos Anjos Lima, Chavarette, dos Santos e Souza, Silva Frutuoso de Souza, and Martins Lopes (2014), among others.

It is important to emphasize that the monitoring and identification of structural failures is a complex problem and is much-discussed in the literature. Thus, it is important to develop new tools to contribute with new alternatives, even innovative alternatives to solve this type of problem.

The choice of using the AIS through the negative selection algorithm is essentially justified due to it is ability to learn and recognize patterns and to present excellent performance in other types of pattern recognition and diagnosis problems, as high - lighted by the authors em F. P. Lima, Chavarette, Souza, and Lopes (2017); Merizio, Chavarette, and Outa (2019).

The ClonalG algorithm works in 8 steps, starting with the selection of a specific population of antibodies that are cloned and hypermutated for further evaluation of the affinity between these and the antigens. Followed by the re-selection process, the best clones are selected to be evaluated and mutated in order to obtain the best possible combination of antigen and antibody De Castro and Von Zuben (2000). ClonalG is commonly applied in domains of optimization and pattern recognition, being therefore chosen.

In comparison with the works of F. P. Lima et al. (2017); Oliveira, Chavarette, and Lopes (2019), the differential of this work is the optimization using genetic algorithm; the clonal selection algorithm. In this case, approximately 50% less data is needed in the training phase than the algorithm without optimization. In addition, the system is capable of identifying and any type of failure, due to the capacity for continuous learning. A failure never before presented to the system can be identified as a new failure pattern, for future identification and localization.

Compared to the work published by Chouidira, Khodja, and Chakroune (2019), this work differs in that it does not require any pre-modeling of the system, being able to adapt to different situations and systems. For example, this same algorithm was applied in the detection of faults in pipes by acoustic means, with few modifications, by the authors Merizio, Chavarette, Moro, Outa, and Mishra (2021).

Compared to the article published by Eren (2017), which uses the same database as this research, this article differs in terms of the method used. AIS are more efficient in detecting and locating faults for this type of application, as the results suggest, requiring less data in training and presenting more satisfactory results than in the article by the mentioned authors.

II. MATERIALS AND METHODS

Pattern recognition, studied by authors such as Hunt, Timmis, Cooke, Neal, and King (1999), Forrest, Javornik, Smith, and Perelson (1993) and Dasgupta and Forrest (1999), is one among several applications of Artificial Immune Systems (AIS). This computationally elaborated tool is based on the ability of the biological immune system to identify antigens and antibodies and decide how to perform the interaction between them.

The AIS and the Clonal Selection Algorithm are composed of intelligent methodologies, inspired by the biological immune system, for solving real world problems Dasgupta and Nino (2008).

In the development of genetically inspired algorithms it is not appropriate to attempt partial or total reconstruction of the immune system. It is more appropriate to use the path of developing pragmatic models inspired by the immune system, preserving the primary biological characteristics that are amenable to computational implementation and effective in the development of engineering tools Castro, De Castro, and Timmis (2002a); Hunt et al. (1999).

2.1 Artificial Immune System (AIS)

The proposed SHM system is based on AIS, especially on the Negative Selection Algorithm. The Negative Selection Algorithm (NSA) was proposed by Forrest, Perelson, Allen, and Cherukuri (1994), to detect changes in states of computational systems. This technique is inspired by the process of negative selection of T lymphocytes, which occurs in the thymus, this process represents the discrimination that the

organism performs with the cells of the body, between them proper cells and non-proper cells.

The NSA's technique is based on the pattern recognition exerted by the biological immune system in the recognition of T lymphocytes that occurs in the thymus

F. P. Lima, Lopes, Lotufo, and Minussi (2016); Merizio et al. (2020). The diagnostic system of the algorithm consists of two phases: The Censor phase and Monitoring; as illustrated and shown by Fig. 1.

In the Censor phase, sets of detectors are created. This set of vectors will constitute the baseline, which stores the normal operating data of the system and will be used later by the AIS to detect failures in real time comparing it with the rotor data, discriminating own/non-own signals, in the Monitoring. Random strings are chosen, starting from reading the data. Detectors function as mature T-type cells that have the ability to recognize pathogens, that is, the ability to detect almost every non-self element Castro et al. (2002a); F. P. Lima et al. (2016).

In the censorship module, as shown on the left in Fig. 1, a signal is chosen at random and has its correspondence checked with the baseline. If the affinity between these is higher than the calculated affinity rate, the signal is rejected and a new signal is analyzed, otherwise the signal is stored at the set of damage detectors F. P. Lima et al. (2016); Outa et al. (2020).

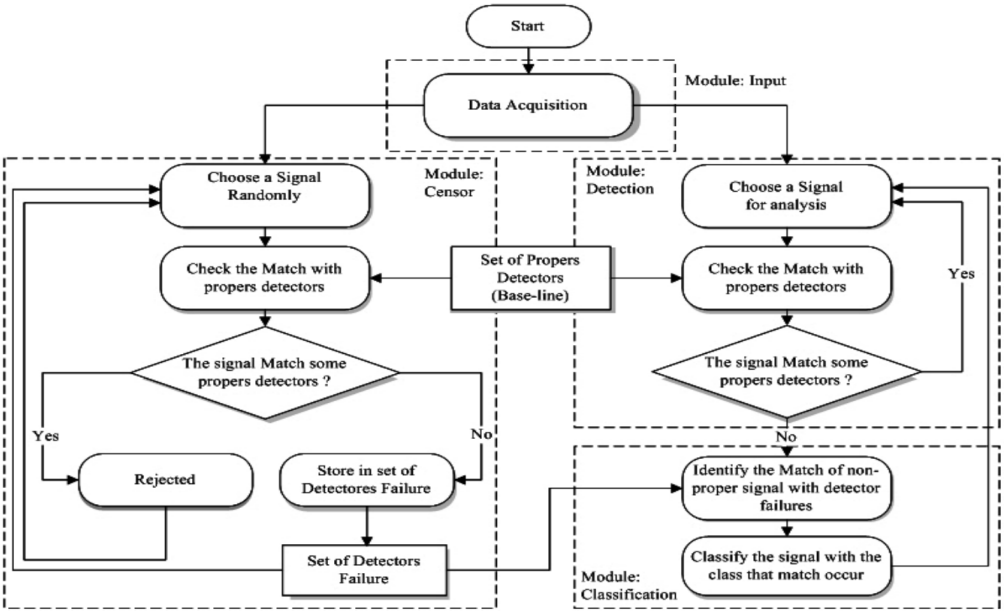

Figure 1: Flowchart of the censo phase and monitoring of the NSA. From Parra dos Anjos Lima, Chavarette, Silva Frutuoso de Souza, et al. (2014)

In this work, ClonalG was applied precisely in the Censoring Module stage, generating new signals based on those provided for the analysis, in order to insert greater diversity into the system. That is, the baseline is not exactly composed by the structure's signals, but by the antibodies generated by ClonalG that have better affinities with the antigens provided by the NSA in the first stage.

To the right of the Fig. 1, after the acquisition of the signals, the detection module is executed, where the signals being analyzed are compared with the own detectors, performing to analyze the marriage between the signals. If the signal is close enough to the baseline (affinity higher than the calculated affinity rate), the system skips to the next signal. Otherwise, an abnormal situation is detected and this signal will go to the classification module F. P. Lima et al. (2017); Merizio et al. (2020).

Finally, in the classification module, the signals selected in the previous step are compared with the damage detectors, in order to perform the signal classification F. P. Lima et al. (2017).

The match ratio (TAf) represents the degree of similarity necessary for match to occur between two chains under analysis. It is defined according to the following equation 1 Oliveira et al. (2019); Outa et al. (2020):

$$TAf = \frac{An}{At} * 100 \quad (1)$$

Where:

TAf : match ratio;
An: number of normal chains in the problem (proper chains);
At: total number of chains in the problem (proper and nonproper chains).

Is used to analyze the affinity between signals and to verify if there similarity/equality the criterion known as marriage, that can be perfect or partial.

A partial match occurs when a predetermined amount of positions between signals has the same value. This amount is called the affinity rate. A perfect match occurs when all signal positions have the same values, is both are perfectly equal Merizio et al. (2019).

In this work was use the partial marriage criterion proposed by Bradley and Tyrrell (2002) and a 12% deviation in the proper detectors.

2.2 Clonal Selection Algorithm

The adaptive immune response is the base of the Clonal Selection Algorithm (ClonalG), originally proposed by De Castro and Von Zuben (2000). The affinity maturation process and the principle of clonal selection proportional to affinity are the pillars of ClonalG's work.

When a human with non-defective adaptive immunity is exposed to an antigen, some his cells subpopulations, derived from bone marrow, called B lymphocytes, respond by producing antibodies (Ab). Each cell secretes only one type of antibody, which is specific for the antigen. The antigen connects with the B lymphocyte receptor and, after a second signal from accessor cells (such as the TH cell), the antigen stimulates the B cell to divide and turn into terminal cells of the type secretory of antibodies, called plasma cells De Castro and Von Zuben (2000); De Oliveira, Chavarette, and dos Anjos Lima (2020).

As De Castro and Von Zuben (2000) says, in ClonalG the maintenance of memory cells works independently of the repertoire. With the most stimulated cells, selection and repro- duction (cloning) occurs. For the least stimulated cells, only death. Then, with clones with higher antigenic affinities, affinity maturation and hypermutation proportional to cell affinity occur. After this process, these clones are re-selected and re-added to the initial group, on condition that it respect the maintenance of the group's diversity.

The CLONALG for recognition problems and machine learning has the following steps, as shown in Fig. 2.2 Castro, De Castro, and Timmis (2002b); De Oliveira et al. (2020); F. P. Lima et al. (2016):

1. *Initiation:* Is randomly generated the population of antibodies (Ab) composed of Ab = Ab{m} + Ab{r} with N lymphocytes for each of the antigens (Agj), where N is the sum of M plus R;
2. *Affinity rating:* Is determined an affinity vector between each (Agj) and the lym- phocytes in the population (Ab).
3. *Selection:* Aiming to compose a subpopulation Abj {n} ulation Ab the n antibodies with greater affinities;, are removed from the population *Ab* the *n* antibodies with greater affinities;
4. *Cloning:* The selected antibodies will proliferate (cloning) in proportion to them affinities with the antigen, generating a new set C of clones. The greater the affinity f, the greater the number of clones of each of the selected lymphocytes;
5. *Hypermutation:* Then, the C population of clones is subjected to the affinity maturation process generating a new population C*, where each antibody will undergo a mutation with a rate inversely proportional to its affinity: the greater the affinity, lower will be the mutation rate;
6. *Affinity rating:* A new vector f* is generated to comparing the set C* and the antigens (Agj);

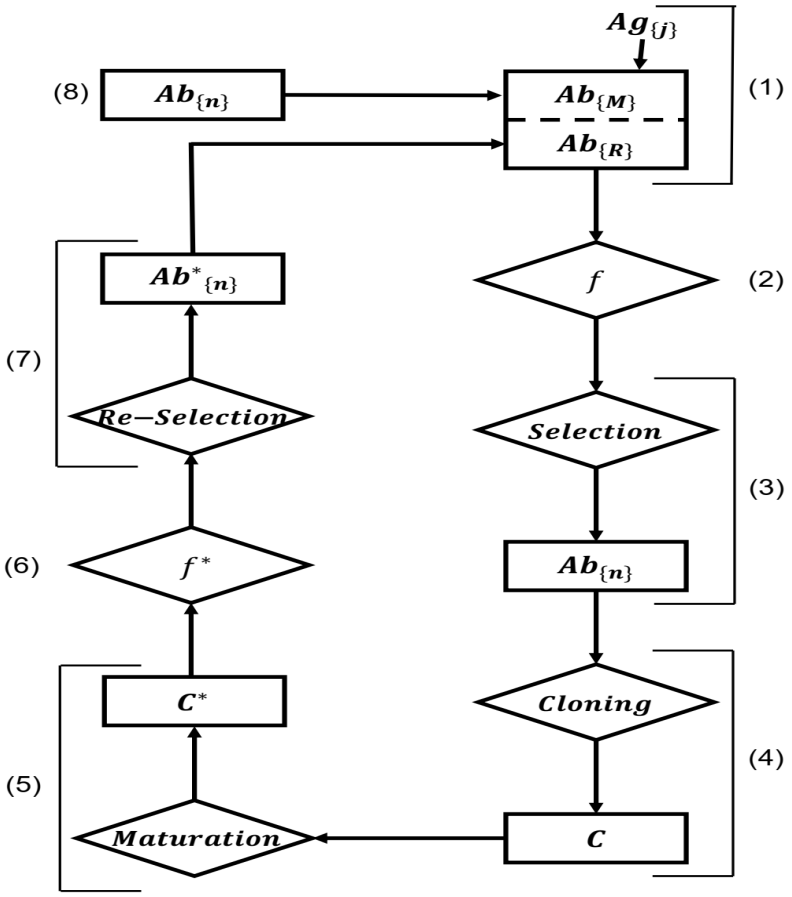

Figure 2: Flowchart of the Clonal Selection Algorithm for the pattern recognition problem

7. *Re-selection:* From this mature population C*, re-select the n best antibodies, the subset Ab{n}, in order to be candidates for entering the memory set Ab{m}. One lymphocyte will be able to enter in the memory set when it has higher affinity rates than another memory lymphocyte inside the set, replacing it;
8. *Metadinamics:* D of the antibodies with lower affinities of R are chosen to be replaced by D new individuals, inducing diversity in the repertoire.

The process from steps 2 to 8 is repeated until the stop criterion is reached.

M sensors with high affinity rates with the presented antigen population Ag(i). This After the stop criterion is satisfied, the set of memory lymphocytes Ab{m} have select group will be used by the NSA in the detection and classification of antigens.

Clonal G was implemented in the NSA censorship module after the signals be selected randomly in the initial phase, with (Agj) antigens entering in the ClonalG. What the NSA receives from ClonalG to make the classification is precisely the population of Ab antibodies.

II. DESCRIPTION OF THE TEST RIG SETUP

The database used was collected by the NSF I/URC Center for Intelli- gent Maintenance Systems (IMS – www.imscenter.net) and is available on the NASA website (https://ti.arc.nasa.gov/tech/dash/groups/pcoe/prognostic-data-repository/) entitled Bearing Data Set.

The experimental table consists of a shaft connected to an AC motor with constant speed (2000 RPM) where 4 oil-lubricated double roller bearings (Rexnord ZA-2115) are installed. On the 2 central bearings a radial load of 6000 lbs is applied by a spring mechanism. Four highly sensitive accelerometers are used for data set. In Fig. 3 it is possible to see the diagram of the rotor.

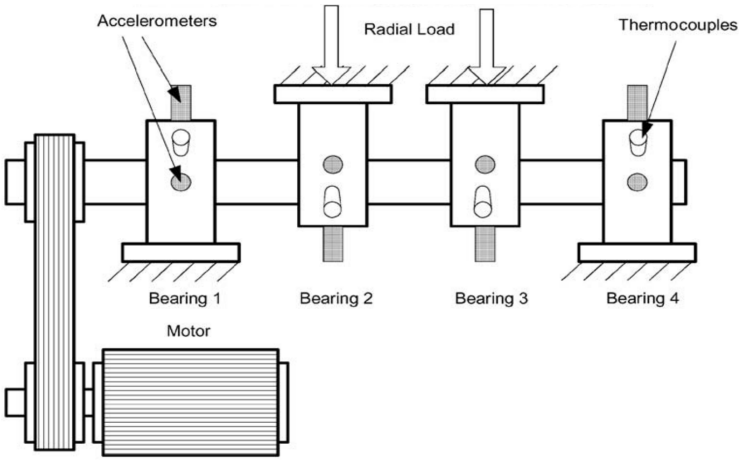

Figure 3: Bearing test rig and sensor placement illustration. From Qiu et al. (2006)

The data set was collected using PCB 353B33 High Sensitivity Quartz ICP accelerometers installed one on each bearing. The failures are expected after exceeding the life of the bearing project, with more than 100 million revolutions. Data collection was facilitated by NI DAQ Card 6062E Qiu et al. (2006).

Data were collected from an experimental table. The experiment was run until one of the bearings failed, which occurred after approximately 44 days. The vibration data is collected at 20 kHz for a second from accelerometers installed on each bearing housing once every twenty minutes. The data has 20,480 points at each recording with sampling rate of 20 kHz. The proposed bearing failure detection algorithm is applied to the collected data. The failure occurred in bearing 3, which develops an outer race defect.

The choice of applying the algorithm to the data collected from the lubricated bearings is due to this being a classic and well-known dynamic vibrational set, which further enables the ability to generate the system for more specific dynamic applications.

IV. RESULTS

4.1 AIS without optimization

From the application of the AIS in the database for fault detection, the following results were obtained: Of the 6321 experimental collections, the rotor was detected in a normal situation in 6076 of them. 6066 is the right number of normal signals. The signs identified as failure were: 6002, 6068 to 6107, 6109 to 6128, 6130 to 6134,6136, 6137 and 6144 to 6319. Of these, 1 is the number of false positives and 11 the number of false negatives. That is, the system issued a fault alert on signal 6002, which should be classified as a normal signal, and 11 fault signals were classified as normal. The hit rate of the AIS was 99.922%, using a affinity rate calculated of 95.98%. 5.0% of normal signals were used to compose the baseline, with 2.0% deviation over each signal; as explained by Bradley and Tyrrell (2002); F. P. Lima et al. (2016) the proposed deviation is adopted in order to make the process more dynamic and efficient. In contrast, the higher the deviation, the higher the risk adopted. Deviations between 0.5% and 10% are commonly adopted.

The catastrophic system failure occurred on March 17 at 8 pm and 22 minutes, and the first failure alert was issued at signal 6068 (on March 16 at 8 am and 2 minutes), followed by 39 other alerts (more that 6 consecutive hours of alert), in other words: The first real fault alert was issued more than 36 hours before the system stopped. The first ”false failure” signal was issued 17 hours before detection by AIS.

The Tab. 1 table shows the percentages of affinity between each signal and the baseline. Signals 1000 to 1001 are an example of AIS's behavior in classifying normal signals, while signs from 6068 to 6072 are examples of classification that AIS detected as a failure and from 6289 onwards the catastrophic failure occurred.

Table 1 shows how high the affinities are, and higher than the affinity rate, in normal signals, and the affinity reduction behavior the closer the fault is.

4.2 AIS with ClonalG optimization

ClonalG was developed and applied in the NSA Censor phase. As stated in Section 2, the ClonalG algorithm finds the lymphocytes that are closest to the antigens provided by the system. In other words, ClonalG identifies the curves as close as possible to the structure data under normal conditions.

Figure 4.2 presents the convergence graph of ClonalG in the NSA Censor phase, where it can be seen that after 25 iterations, there are no major changes in convergence (absolute distance between the antibodies and the antigens presented).

The application of ClonalG to optimize the NSA generated the following results: From the universe of 6321 data collections, the rotor was detected in a normal situation in 6077. Faults were detected between signals: 6068 to 6081, 6083 to 6119, 6121 to 6131, 6133 to 6137 and 6144 to 6319. Of the signs mentioned, there were no false positives and there were 11 false negatives. As a final result, the fault detection accuracy increased to 99.928%.

That is, an improvement of less than 0.01%. However, the use of ClonalG allows important changes in the NSA parameters, for example: There was a 50% reduction in the percentage of normal signals used to compose the base-line, previously 5% of normal signals were used, 2.5% are now used. Besides that, there was 70% reduction in the deviation used, before it was 2% and now the percentage has been reduced to 0.6%. Physically, the use of less data by the NSA directly means greater robustness of the AIS, and the use of a smaller deviation provides greater security in operations.

The cost of this greater reliability is the need more processing power and available memory, and the algorithm optimized with ClonalG can take up to 68% more time than the previous one to complete the processing on the same hardware.

Table 2 shows the affinities between signal and the lymphocytes indicated by Clon- alG in the Censor phase of the NSA.

Comparing Tab. 2 with Tab. 1, it can be verified that there were practically no changes between the two cases. This is justified due to the size of the data set and the ratio of normal signals to the number of total signals be high. When using better data set, the affinities found by the optimized system are slightly higher than before.

Table 1: Affinities calculated by AIS for each signal in relation to baseline

Signal number	Position 1 (%)	Position 2 (%)	Position 3 (%)	Position 4 (%)
1000	99.80	99.12	99.41	99.51
1001	99.61	99.61	99.90	99.41
1002	99.80	99.32	99.32	99.80
1003	99.80	99.02	99.61	99.12
1004	98.63	99.51	99.32	99.32
1005	98.04	99.12	98.83	98.73
1006	99.22	99.32	99.71	99.80
1007	99.80	99.90	99.80	99.41
1008	99.90	99.71	99.71	99.32
1009	99.41	99.90	99.51	99.12
6068	99.71	99.02	94.33	95.99
6069	99.61	99.12	95.11	97.65
6070	99.12	99.12	93.55	96.48
6071	99.41	99.12	95.11	96.38
6072	99.51	99.61	95.01	96.48
6289	99.02	95.60	79.08	98.14
6290	99.61	98.44	74.68	94.04
6291	95.70	85.43	61.39	69.89
6292	88.37	87.00	37.73	88.37
6293	86.31	86.02	35.48	87.59

4.3 Failure location by AIS

The fault location was performed using the minimum deviation method. The median of standard deviations was calculated, which was calculated from the failure signals detected in relation to the baseline.

Table 3 shows the respective calculation for each sensor.

The higher the result, the higher the distance between the values of the signals from that position in relation to the values in the same position of the baseline and the closer the fault accelerometer is. AIS correctly identified the location of the failure in the case presented in position 3. When applying the same method to others data set with others fault positions, AIS has always identified the location of the failure with an excellent safety margin.

As an example of that described, Tab. 4 presents the results of the fault location for another data set of a rotor also with 4 bearings and 4 accelerometers, where the fault is in position 1. Being correctly identified by the AIS.

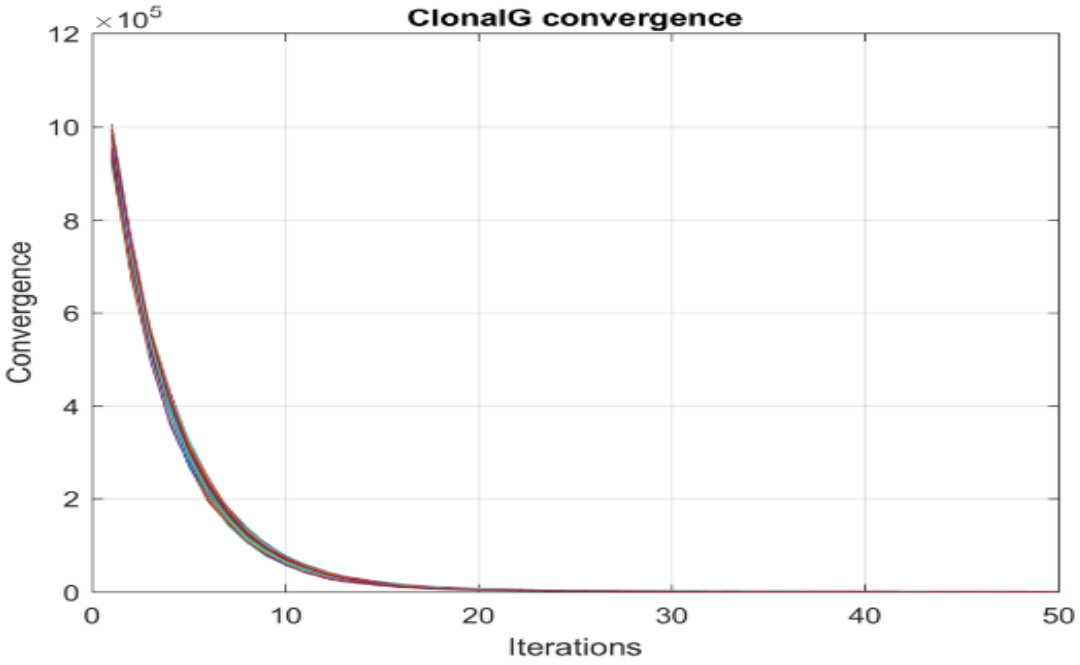

Figure 4: ClonalG convergence graph

V. CONCLUSIONS

The failure detection performed by the AIS based on the NSA was able to predict the occurrence of the failures with a good safety margin. The application of this type of technique in the monitoring of the health of instrumented dynamic systems allows a greater use of the useful life, indicating what is the best time to carry out the replacement without accidents occurring.

The AIS obtained a hit rate of 99.992%, issuing 1 false positive and 11 false neg- atives, of a total of 6321 signals. The predictability of the failure occurring started more than 36 hours before the system stopped. In the case of optimized AIS, the hit rate increased by less than 0.01%, due to the non-detection of the false positive.

Although there are no relevant changes in the overall success rate of the AIS, it can be considered that with the optimization of the SHM by ClonalG interesting results were obtained, in the sense of there a 50 % reduction in the need for training data. Before, the system needed to know 5.0% of the normal signals in the Censor phase and, after the optimization, this number increased to 2.5%. As well as a reduction of 70% in the deviations used, being considerable reductions, which show a good optimization by the Clonal selection mechanism.

The fault location by the method of minimum deviations was successful, with more than 75% reliability in all cases analyzed (considering the distance between the deviations of the accelerometers with and without failure).

Genetic algorithms proved to be an interesting tool in the monitoring of structures used in Mechanical Engineering, being a robust and reliable method for the detection and localization of failures.

Table 2: Affinities calculated by AIS for each signal in relation to the lymphocytes selected by ClonalG

Signal number	Position 1 (%)	Position 2 (%)	Position 3 (%)	Position 4 (%)
1000	99.90	99.71	99.71	99.90
1001	99.71	99.61	99.71	99.80
1002	99.80	99.51	99.51	99.71
1003	99.71	99.90	99.71	99.71
1004	99.90	99.71	99.61	99.90
1005	99.80	99.12	99.41	99.61
1006	99.71	99.80	99.90	99.32
1007	99.61	99.80	99.51	99.12
1008	98.83	99.51	98.83	99.41
1009	99.90	99.12	98.83	98.83
6068	99.22	99.22	94.92	96.68
6069	99.80	99.41	95.01	97.65
6070	99.32	99.02	93.84	96.87
6071	99.51	99.02	94.92	96.58
6072	99.71	99.51	95.01	95.21
6289	98.92	96.29	79.86	98.44
6290	99.61	98.63	75.17	94.13
6291	96.19	89.35	64.42	73.22
6292	91.30	91.40	43.60	91.79
6293	87.39	88.47	37.24	89.54

Table 3: Fault location using the minimum deviations method

Position 1 (%)	Position 2 (%)	Position 3 (%)	Position 4 (%)
68.230	95.571	437.560	104.516

ACKNOWLEDGEMENTS

This work was supported by the S˜ao Paulo Research Foundation (FAPESP) under Grant 2018/16447-8 and 2019/10515-4; and National Council for Scientific and Technological Development under Grant 312972/2019-9; The authors thank the Universidade Estadual Paulista ”Julio de Mesquita Filho” and the Laboratory of Complex Systems (SisPLEXOS) for the space provided.

Disclosure statement

The authors declare that they have no conflict of interest.

Table 4: Fault location performed in another data set

Position 1 (%)	Position 2 (%)	Position 3 (%)	Position 4 (%)
292.497	51.211	59.476	38.194

Data availability statement

The data used are available at:https://ti.arc.nasa.gov/tech/dash/groups/ pcoe/prognostic-data-repository/.

REFERENCES

1. Abreu, C., Chavarette, F., Villarreal, F., Duarte, M., & Lima, F. (2014). Dual-tree complex wavelet transform applied to fault monitoring and identification in aeronautical structures. International Journal of Pure and Applied Mathematics, 97 (1), 89 – 97.
2. Bradley, D. W., & Tyrrell, A. M. (2002). Immunotronics-novel finite-state-machine architectures with built-in self-test using self-nonself differentiation. IEEE Transac- tions on Evolutionary Computation, 6 (3), 227–238.
3. Castro, L. N., De Castro, L. N., & Timmis, J. (2002a). Artificial immune systems: a new computational intelligence approach. Springer Science & Business Media.
4. Castro, L. N., De Castro, L. N., & Timmis, J. (2002b). Artificial immune systems: a new computational intelligence approach. Springer Science & Business Media.
5. Chandrashekhar, M., & Ganguli, R. (2009). Structural damage detection using modal curva- ture and fuzzy logic. Structural Health Monitoring, 8 (4), 267–282.
6. Chen, H., Yan, Y., Chen, W., Jiang, J., Yu, L., & Wu, Z. (2007). Early damage detection in composite wingbox structures using hilbert-huang transform and genetic algorithm. Structural Health Monitoring, 6 (4), 281–297.
7. Chouidira, I., Khodja, D., & Chakroune, S. (2019). Induction machine faults detection and localization by neural networks methods. Rev. d'Intelligence Artif., 33 (6), 427–434.
8. Dasgupta, D., & Forrest, S. (1999). Artificial immune systems in industrial applications. In Proceedings of the second international conference on intelligent processing and manufacturing of materials. ipmm'99 (cat. no. 99ex296) (Vol. 1, pp. 257–267).
9. Dasgupta, D., & Nino, F. (2008). Immunological computation: theory and applications. CRC press.
10. De Castro, L. N., & Von Zuben, F. J. (2000). The clonal selection algorithm with engineering applications. In Proceedings of gecco (Vol. 2000, pp. 36–39).
11. De Oliveira, D. C., Chavarette, F. R., & dos Anjos Lima, F. P. (2020). Structural health monitoring using artificial immune system/ monitoramento estrutural da sau´de usando sistema imunol´ogico artificial. Brazilian Journal of Development , 6 (4), 16948–16963.
12. Eren, L. (2017). Bearing fault detection by one-dimensional convolutional neural networks. Mathematical Problems in Engineering, 2017 .
13. Flynn, E. B., & Todd, M. D. (2010). Optimal placement of piezoelectric actuators and sensors for detecting damage in plate structures. Journal of Intelligent Material Systems and Structures, 21 (3), 265–274.
14. Forrest, S., Javornik, B., Smith, R. E., & Perelson, A. S. (1993). Using genetic algorithms to explore pattern recognition in the immune system. Evolutionary computation, 1 (3), 191–211.
15. Forrest, S., Perelson, A. S., Allen, L., & Cherukuri, R. (1994). Self-nonself discrimination in a computer. In Proceedings of 1994 ieee computer society symposium on research in security and privacy (pp. 202–212).
16. Giurgiutiu, V., & Cuc, A. (2005). Embedded non-destructive evaluation for structural health monitoring, damage detection, and failure prevention. Shock and Vibration Digest , 37 (2), 83.
17. Hall, S. (1999). The effective management and use of structural health data. In Proceedings of the 2nd international workshop on structural health monitoring (pp. 265–275).
18. Hunt, J., Timmis, J., Cooke, E., Neal, M., & King, C. (1999). Jisys: the envelopment of an artificial immune system for real world applications. In Artificial immune systems and their applications (pp. 157–186). Springer.
19. Lima, F., Lotufo, A., & Minussi, C. (2013). Artificial immune systems applied to voltage disturbance diagnosis in distribution electrical systems. In 2013 ieee grenoble conference (pp. 1–6).
20. Lima, F. P., Chavarette, F. R., Souza, S. S., & Lopes, M. L. (2017). Monitoring and fault identification in aeronautical structures using an wavelet-artificial immune system algorithm. In Probabilistic prognostics and health management of energy systems (pp. 203–219).

21. Springer. Lima, F. P., Lopes, M. L., Lotufo, A. D. P., & Minussi, C. R. (2016). An artificial immune system with continuous-learning for voltage disturbance diagnosis in electrical distribution systems. Expert systems with applications, 56 , 131–142.
22. Lopes Jr, V., Turra, A., Mu¨ller, H., Brunzel, F., & Inman, D. (2001). A new methodology of damage detection by electrical impedance and optimization technique. In Conference on dynamic problem in mechanics–diname (Vol. 13, pp. 311–316).
23. Merizio, I. F., Chavarette, F. R., Moro, T. C., & Outa, R. (2020). Fault detection by acoustic means using the negative selection algorithm. In Colloquium exactarum. issn: 2178-8332 (Vol. 12, pp. 61–70).
24. Merizio, I. F., Chavarette, F. R., Moro, T. C., Outa, R., & Mishra, V. N. (2021). Machine learning applied in the detection of faults in pipes by acoustic means. Journal of The Institution of Engineers (India): Series C , 1–6.
25. Merizio, I. F., Chavarette, F. R., & Outa, R. (2019). Characterization of an acoustic impedance tube using natural computer. In Colloquium exactarum. issn: 2178-8332 (Vol. 11, pp. 62– 72). DOI: 10.5747/ce.2019.v11.n4. e297.
26. Oliveira, D. C., Chavarette, F. R., & Lopes, M. L. (2019). Damage diagnosis in an isotropic structure using an artificial immune system algorithm. Journal of the Brazilian Society of Mechanical Sciences and Engineering , 41 (11), 1–11.
27. Outa, R., Chavarette, F. R., Mishra, V. N., Gon¸calves, A. C., Roefero, L. G., & Moro, T. C. (2020). Prognosis and fail detection in a dynamic rotor using artificial immunological system. Engineering Computations.
28. Pandey, P., & Barai, S. (1995). Multilayer perceptron in damage detection of bridge structures. Computers & structures, 54 (4), 597–608.
29. Parra dos Anjos Lima, F., Chavarette, F. R., dos Santos e Souza, A., Silva Frutuoso de Souza, S., & Martins Lopes, M. L. (2014). Artificial immune systems with negative selection applied to health monitoring of aeronautical structures. In Advanced materials research (Vol. 871, pp. 283–289).
30. Parra dos Anjos Lima, F., Chavarette, F. R., Silva Frutuoso de Souza, S., dos Santos e Souza, A., & Martins Lopes, M. L. (2014). Artificial immune systems applied to the analysis of structural integrity of a building. In Applied mechanics and materials (Vol. 472, pp. 544–549).
31. Pita, J. L., Turra, A. E., & Vieira Filho, J. (2013). Detec¸c˜ao de danos em tubula¸c˜oes usando a t´ecnica baseada na imped^ancia eletromec^anica (emi). Proceeding Series of the Brazilian Society of Computational and Applied Mathematics, 1 (1).
32. Qiu, H., Lee, J., Lin, J., & Yu, G. (2006). Wavelet filter-based weak signature detection method and its application on rolling element bearing prognostics. Journal of sound and vibration, 289 (4-5), 1066–1090.
33. Santiago, D. F. d. A., et al. (2004). Diagn´ostico de falhas em m´aquinas rotativas utilizando transformada de wavelet e redes neurais artificiais.
34. Tebaldi, A. (2004). Detec¸c˜ao de falhas estruturais usando sensores e atuadores piezel´etricos e algoritmos gen´eticos.
35. Zheng, S., Wang, X., & Liu, L. (2004). Damage detection in composite materials based upon the computational mechanics and neural networks. In European workshop on structural health monitoring, munich (pp. 609–615).

This page is intentionally left blank

Analysis of AISI 316 Steel Surface in Turning Process using Vegetable Oils

Hellen Cristina Pires Souza & Antonio Santos Araujo Junior

ABSTRACT

The use of cutting fluids aims to meet the needs of cooling and lubrication during the material removal process. Therefore, the present work sought to investigate the results regarding the quality of the surface finish of AISI 316 steel, using a complete factorial planning (DOE - Design of Experiments) of 03 factors in 2 levels (23), considering input speed, feed and depth of cut and 01 qualitative factor, which are vegetable cutting fluids (commercial - quimatic, cotton and canola) and also in the dry condition, using for pliation the technique of the Minimum Amount of Fluids (MQF) with a flow of 90 ml/h, totaling 32 tests, analyzed for their effects of mean roughness (Ra). The results showed that vegetable oils presented roughness close to commercial oil, which demonstrates a potentiality as alternatives for replacing commercial cutting fluids.

Keywords: factorial planning, machining, roughness.

Classification: DDC Code: FIC LCC Code: PZ7.W996

Language: English

London Journals Press

LJP Copyright ID: 392943
Print ISSN: 2631-8474
Online ISSN: 2631-8482

London Journal of Engineering Research

Volume 22 | Issue 3 | Compilation 1.0

Analysis of AISI 316 Steel Surface in Turning Process using Vegetable Oils

Hellen Cristina Pires Souza[α] & Antonio Santos Araujo Junior[σ]

ABSTRACT

The use of cutting fluids aims to meet the needs of cooling and lubrication during the material removal process. Therefore, the present work sought to investigate the results regarding the quality of the surface finish of AISI 316 steel, using a complete factorial planning (DOE - Design of Experiments) of 03 factors in 2 levels (23), considering input speed, feed and depth of cut and 01 qualitative factor, which are vegetable cutting fluids (commercial - quimatic, cotton and canola) and also in the dry condition, using for pliation the technique of the Minimum Amount of Fluids (MQF) with a flow of 90 ml/h, totaling 32 tests, analyzed for their effects of mean roughness (Ra). The results showed that vegetable oils presented roughness close to commercial oil, which demonstrates a potentiality as alternatives for replacing commercial cutting fluids.

Keywords: factorial planning, machining, roughness.

Author α σ*:* Programa de Pós Graduação em Engenharia Mecânica – PPGMEC, Laboratório de Usinagem, Departamento de Mecânica e Materiais - DMM, Instituto Federal de Educação, Ciência e Tecnologia do Maranhão-IFMA, CEP.

I. INTRODUCTION

In recent years there has been a greater concern regarding the continuous improvement of methods, processes and technical aspects of manufactured products. In its entirety, mechanical manufacturing processes currently seek the best adaptation between machine and tool to obtain a better quality and productivity. In this way, machining manufacturing processes are essential in the mechanical metal industry, as most products undergo some machining operation in some of their production stages. The DIN 8560 standard[1] defines that machining is the manufacturing process that gives the part shape, dimensions, finish or even a combination of any of these three, through the removal of material in the form of chip material part of the part removed by the cutting tool, characterized by an irregular shape.

By analyzing the environmental aspects of machining operations, it is possible to identify several sources that are aggressors to the environment, including cutting fluids or lubri-refrigerant fluids, which are used in large quantities to increase the life of the tools and improve the quality of the parts produced[2]. Conventional cutting fluids that are used to ease the wear of cutting tools and increase their service life pollute the environment and produce diseases to professionals in contact with these fluids. Therefore, the use of vegetable oils appears as a good option in place of petroleum products, since they are less harmful to the environment, biodegradable, renewable and less toxic[3]. Figure 1 shows the environmental aspects related to the use of cutting fluids in machining processes.

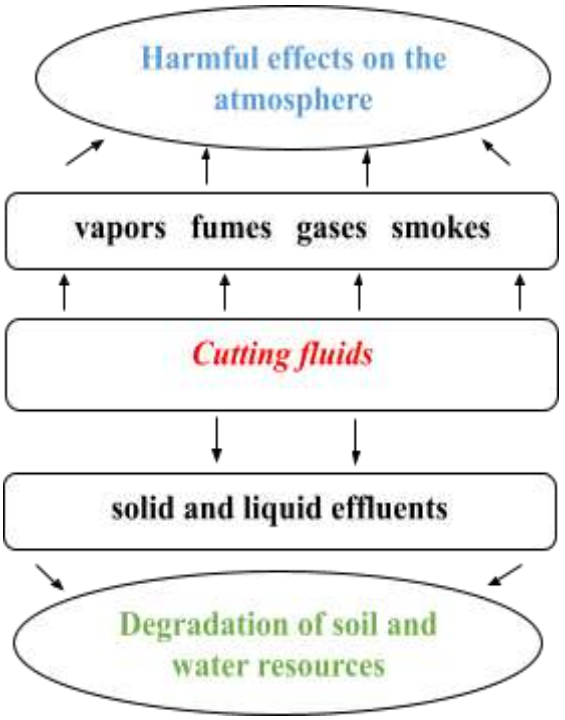

Source: Adapted from ARAÚJO JÚNIOR [2]

Figure 1: Finish rating of machined surface

In this way, there is a high trend towards environmental concerns caused by the use of cutting fluids in machining processes and strong emphasis today is given to environmentally correct technologies, such as dry machining[2].

On the other hand, despite persistent attempts to completely eliminate the use of cutting fluids, in many cases cooling is still indispensable to achieve economically viable tool lives and required surface qualities, such as machining difficult to machine materials and manufacturing components that require high dimensional accuracy[4].

According to SHAW[5], the quality of a machined surface is one of the most important points to be considered during the machining process.

Surface quality is the term that involves several factors, such as: surface finish and absence of cracks, chemical alteration, thermal damage and residual tenare, besides being the characteristic through which the requirements or metallurgical changes that have developed due to machining such as: Phase transformation, encruamento, grain size, recrystallization, inclusions in the material, among others. To optimize cutting conditions and thus obtain better quality on the surface of the material, cutting speed and feed are the two most important parameters that can be adjusted by the operator. The depth of cut is usually relative to the initial and final diameter of the bar, which should be considered, as the removal rate of the material directly influences the finishing[6].

The most used parameters to quantify roughness in the conventional machining processes are average roughness (R_a), total roughness (R_t) and maximum roughness (R_y). The average roughness is applied in most manufacturing processes, it is also known as Ra (roughness average) or CLA (center line average) which means center of the midline[7]. The mean roughness (R_a) is defined as the arithmetic mean of the absolute values of the variables of the distance orders nothings (y), of the points of the roughness profile in relation to the midline within the measurement path (lm). Figure 2 shows this magnitude at the length of a measurement path[8].

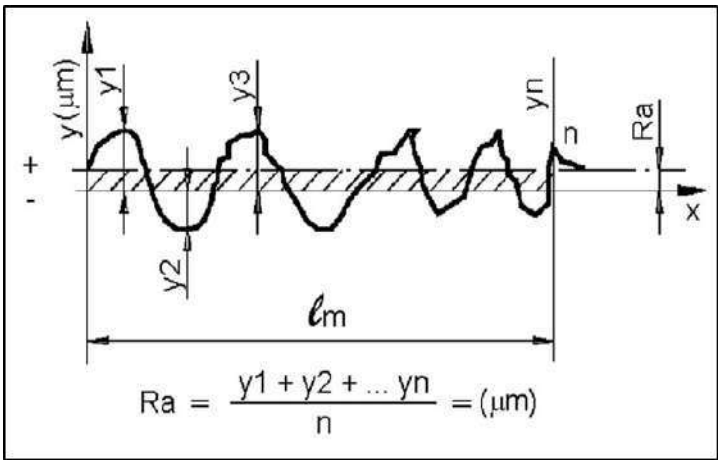

Source: Adapted from NOGUEIRA [7]

Figure 2: Average roughness (Ra)

Given the scenario exposed, the objective of this research was to analyze the fluid effects of plant based cutting, considered environmentally correct, in the process of external cylindrical turning of AISI 316 steel, with application through the MQF method (Minimum Amount of Fluid), to determine through statistical analysis (DOE - Design of Experiments, 2^3) the best technical performance conditions of the machined components through the evaluation of the roughness of the machined surfaces.

II. MATERIALS AND METHODS

2.1 Experimental planning

The experimental planning was elaborated based on a complete factorial planning (2^k) of 03 factors (2^3), establishing relationships with some quantities that involve the machining process, considered as the input variables: cutting speed (v_c), feed (f) and depth of cut (a_p), with variation at two levels each and 01 qualitative factor of comparison: lubri-refrigerants condition, which are:

- Refined vegetable oils of Cotton and Canola;
- Commercial quimatic oil, which is a commercial cutting fluid also ecological and biodegradable, which contains characteristics necessary for application in machining of ferrous metals through the MQF technique;
- Dry condition, i.e. without using any type of lubrirefrigerant.

All oils were applied using the MQF technique, with a flow rate of 90ml/h, performing 8 combined tests for each qualitative condition, totaling 32 trials. The data adopted in the experiment are described in Table 1.

Table 1: Planning matrix for specific roughness measurement machining tests

Variables				
Input				Output
Quantitative			Qualitative	Quantitative
v_c (m/min)	f (mm/rot)	a_p (mm)	Fluids	Roughness Average
75.8	0.173	1.5	Dry; Cotton vegetable fluid; Canola plant fluid; Quimatic commercial fluid	R_a
119.3	0.491	2.0		

2.2 Material specification and cutting tool

The machine tool used in the machinability tests was the universal lathe of the brand NARDINI, model ND 195S, with installed power of 6.12 HP and maximum rotation of 1600 RPM. To perform the machining tests was an AISI 316 steel bar with circular section of 38mm in diameter, which was dismembered into 04 specimens of 200mm in length each, where each specimen was destined to a test condition (dry, with commercial oil, with canola vegetable oil, with cotton vegetable oil). The illustration of the specimens is shown in Figure 4.

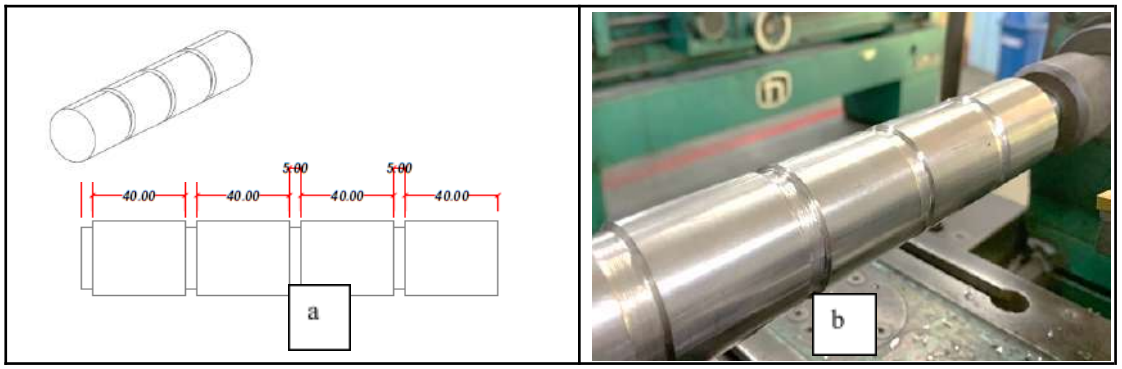

Figure 2: (a) Design of the test body (b) Machined test body

The selection of the material is due to a favorable combination of properties, such as: corrosion and oxidation resistance, hot mechanical resistance, cold workability and weldability.[9] The elements that are part of the chemical composition of austenitic stainless steel AISI 316 are presented in Table 2.

Table 2: Chemical composition steel AISI 316 (in % mass)

Elements	C	Si	Mn	P	S	Cr	Mo	Ni	Al	Co
	Carbon	Silicon	Manganese	Phosphorus	Sulfur	Chromium	Molybdenum	Nickel	Aluminum	Cobalt
Average concentration obtained (%)	0.039	0.46	1.77	0.044	0.024	16.95	2.49	10.9	0.01	0.20
Specification	0.08 Máximo	1.00 Máximo	2.00 Máximo	0.045 Máximo	0.030 Máximo	16.00 - 18.00 Máximo	2.00 - 3.00 Máximo	10,0 - 14,0 Máximo	-	-
Elements	Cu	Nb	Ti	V	W	Pb	Sn	B	N	Fe
	Cuprum	Niobium	Titanium	Vanadium	Tungsten	Lead	Tin	Boron	Nitrogen	Iron
Average concentration obtained (%)	0.039	0.46	1.77	0.044	0.024	16.95	2.49	10.9	0.01	0.20

Source: Labteste[9]

The insert used to perform the experimental work was triangular, with 06 (six) cutting edges, model TNMG 160408, with TiAlN cover, nano structured by pvd method (steam physical deposition), CLASS ISO P25M25. For the fixation of the hard metal insert, the MTJNR 2020-K16 support was used, with a shank measurement of 20x20m and a total length of 125mm. The tool carrier used follows the international standardization of the dimensions of tools for turning, being compatible with the interchangeable insert [10].

For the application of fluids in the Form MQF, a micro-lubrication applicator was used, model accu-lube manufactured by ITW Chemical, with operation by means of a continuous flow to

compressed air, adjusted around 6 Kg/cm², and intermittent fluid spray at the frequency of 1 pulse per second, adjusted to the flow of 90ml/h.

2.2 Surface roughness measurement system

The average roughness (R_a) was determined as a function of the mean line M of the roughness profile and the maximum roughness (R_y), defined as the highest value of partial roughness (Z_i) that is presented in the lm measurement path. They were measured on the machined surface of the part with the aid of a digital rugosimeter model TR220 from TimeGroup Inc., with resolution of 0.01µm and cut-off sampling length (le) of 0.25mm. Roughness was measured in 4 distinct points of the piece, using the midline method – M, as indicated by NBR ISO 4287/2002[11] and NBR 8404/1984[12]. In this system, all quantities are defined from a reference line, the midline, which is defined as a line arranged parallel to the general direction of the profile, within the measurement path, so that the sum of the upper areas, understood between it and the effective profile is equal to the sum of the lower areas. The roughness measurement scheme is shown in Figure 5.

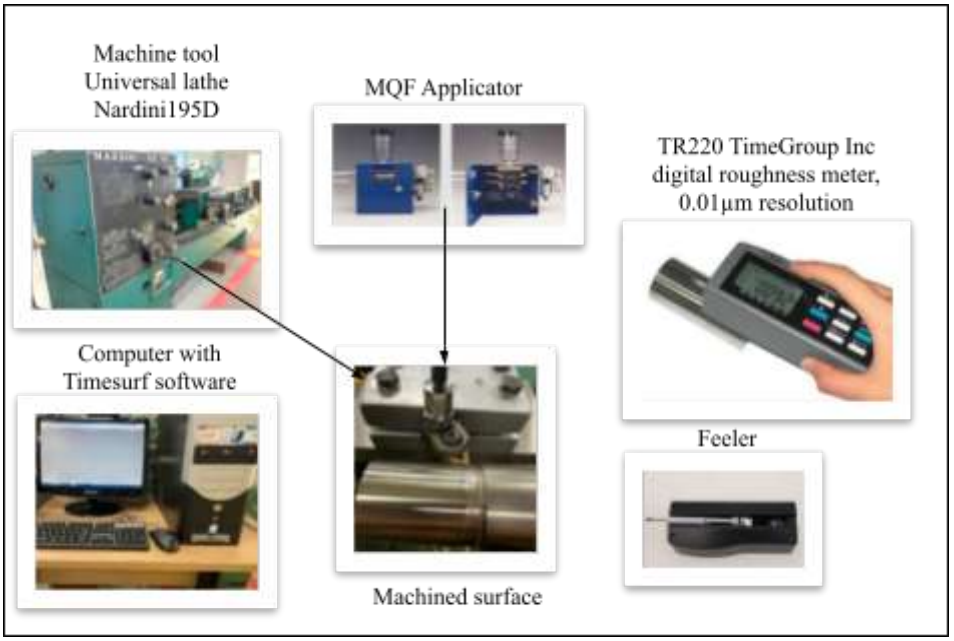

Figure 5: Surface roughness measurement system

III. RESULTS AND DISCUSSIONS

3.1 Effects of cutting parameters on average roughness

Surface roughness influences not only the dimensional accuracy of machined parts, but also their properties, being an important parameter to evaluate the performance of the cutting tool. The irregularity of a surface is the result of the machining process, including the optimal selection of cutting conditions[13]. According to the Pareto chart, shown in Figure 6, it is possible to identify the significant factors and non-significant factors of R_a analysis.

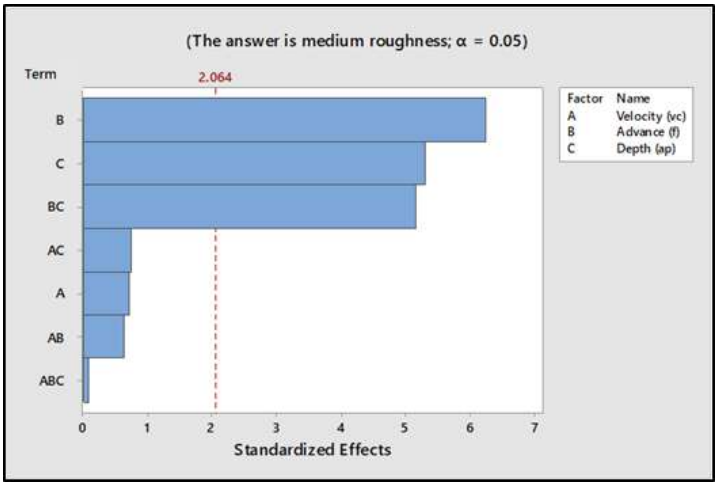

Figure 6: Pareto chart of standardized effects

Adopting a decreasing order we have the advance (f), the depth of cut (a_p) and the interaction between both (f x a_p) as statistically significant, that is, they present values of $p < 0.05$. The other factors contained in the graph are not statistically significant, i.e., the cutting speed (v_c) has little influence on the results obtained. According to Machado and da Silva.[14], advancement is the most influential parameter on roughness, followed by the tool's tip radius. In fact, there was an increase in roughness with the increase in advancement, and it was shown that roughness also increased considerably with increasing depth of cut. Therefore, to achieve lower roughness values, low feed values should be used, associated with low cutting depths, according to the pre-established parameters in factorial planning, which confirms the study presented by Xiao, Liao and Long[15], where the authors mention that when using high advance values, there is a sharp increase in roughness, since the chip tends to be pulled out rather than shear the material.

Therefore, it is important to ratify that proper selection of the advance is essential, because Trent and Wright[16] mention that the reduction of the advance in the turning process reduces the force applied against the cutting tool and in certain cases may compromise the stability of the machine tool system and induce vibrations, thus promoting the reduction of the quality of the surface finish. Kumar, Singh and Singh.[17] mention that several factors influence roughness in the turning process, including lateral chip flow, system vibration, material fixation on the machine, feed and cutting speed. This demonstrates how rough the surface depends on the tool feed (so called feed marks).

3.2 Analysis of the performance of plant fluids in relation to surface finish

The use of cutting fluids also effectively influences the surface finish of tools machined by the turning process, since it promotes a reduction in the machining forces generated and the softening of the vibrations of the machine tool set[2]. Figure 7 graphically shows the behavior of the average roughness (R_a) in relation to variations in cutting conditions and plant and commercial base fluids analyzed.

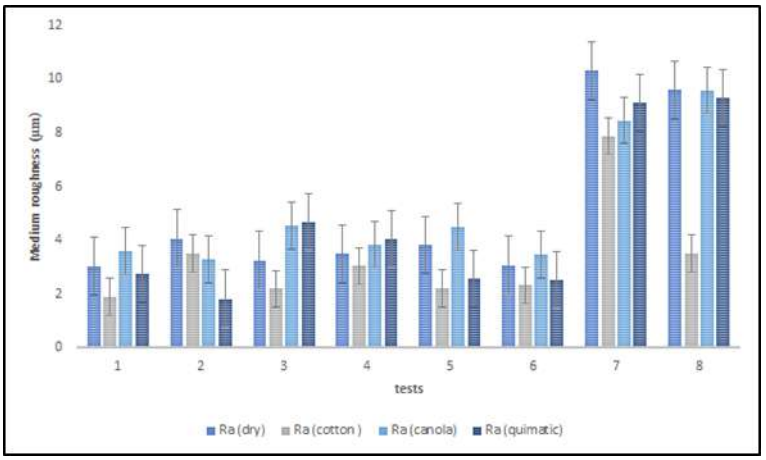

Figure 7: Performance correlations of cutting fluids in relation to average roughness

Figure 7 shows that in all cutting conditions, the dry condition presented the worst desem penho, significantly increasing the surface roughness in terms of R_a, obtaining inadequate surface finishing conditions. Araújo Junior[2] mentions that the good performance applied vegetable oils in the MQF form is justified due to its adequate heat removal and viscosity removal capabilities, which provides a better adhesion of the fluid in the tool part contact area.

To evaluate which vegetable oil presented a better performance in this stage, we used the statistical inference applied to the average roughness criterion, using the student's t-test for paired data (comparison between R_a obtained with application of vegetable oils, with R_a both of the dry condition and with application of the quimatic commercial oil), considering two hypotheses, one being null, where there is no significant difference between the roughness means and the other non-null conside that opposes the first. To define whether the null hypothesis should be rejected or not, a reliability of 95% or equivalently a significance level of 5% was adopted. That is, if the probability of the test (p-value) is less than this significance level, the null hypothesis is rejected. Otherwise, the null hypothesis will not be rejected. This analysis is presented in Table 3.

Table 3: Statistical analysis between vegetable oils in the mean roughness criterion using paired student t hypothesis test at significance level of 5% (α = 0.05)

Vegetable oil	Comparison α=0.05	
	Dry (p-value)	Comercial (p-value)
COTTON	0.032305	0.119406
CANOLA	0.666210	0.115701

When analyzing the comparison regarding the use of vegetable or dry oil, through the paired t-test, it was observed that for the criterion of average roughness (R_a) only cotton oil presents a significant difference between the means obtained (p-value<0.032305<0,05). In the vegetable x commercial comparison (quimatic), there is no significant difference between the means, that is, the type of cutting fluid did not influence the surface roughness.In this case, we chose to use cotton oil, because it presents satisfactory performance when compared to the dry condition and also does not produce harmful consequences for both operators and the environment. Figure 9 illustrates the boxplot graph for comparison between the means obtained in each condition.

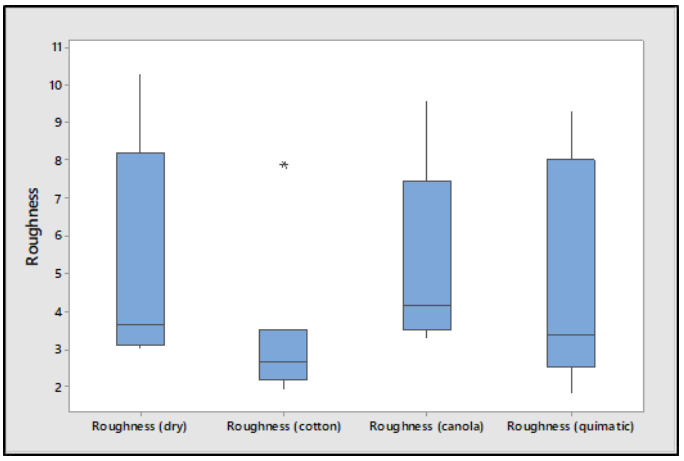

Figure 8: Boxplot for medium roughness (Ra)

Through Figure 8, it can be analyzed that the condition with the use of commercial oil quimatic presented greater variability. In the condition with the use of cotton oil, a superficial finish with lower roughness values was obtained, which confirms the study by Machado and da Silva[16], which reports that for warrant a good performance regarding the surface finish is necessary the appropriate choice of fluid, taking in consideration of the type of metal and the machining parameters.

IV. CONCLUSIONS

The advance proved to be a key parameter in obtaining a good finish in the process of external cylindrical turning of AISI 316 steel. Therefore, for each condition the choice of the correct feed must be made taking into account the material, tool and operation that will be performed on machining.

Cotton oil presented the best performance in relation to the criterion of average roughness (R_a), producing a surface finish of the piece suitable for the cutting conditions studied.

Thus, the use of vegetable cutting fluids proved satisfactory in relation to the superficial quality of the part, and can be used in external cylindrical turning operations, bringing to the industrial process characteristics of biodegradability, exemption from safety and physiological safety for operators. However, one disadvantage that can be pointed out is the presence of oil mist generated by the MQF application process.

ACKNOWLEDGMENTS

The authors thank the Federal Institute of Education, Science and Technology of Maranhão - IFMA and the Graduate Program in Mechanical Engineering - PPGMEC of this Institute for the physical structure and support.

REFERENCES

1. Manufacturing Process – Terms and Definitions (DIN 8560). (2003). Berlin, Germany.
2. Araújo Junior, A. S. (2013). Performance of edible vegetable oils applied by MQF in the front milling of ABNT 1045 Steel. (Doctoral Dissertation). Federal University of Uberlândia, Minas Gerais, Brazil.
3. Alves, S. M., & Oliveira, J. F. G. (2006). Development of new cutting fluid for grinding process adjusting mechanical performance and environmental impact. Journal of Materials Processing Technology. 179(1-3), 185-189. doi:10.1016/j.jmatprotec.2006.03.090.
4. Trend points to dry machining. (2020, 12 04). Retrieved from: http://www.nei.com.br/artig-gos.
5. Shaw, M.C. (2005). Metal Cutting Principles. Oxford University Press, USA.
6. Benardos P.G., & Vosniakos G.C. (2003). Predicting surface roughness in machining: a review. International Journal of Machine Tools & Manufacture. v.43, pp. 833–844, doi: 10.1016/S0890-6955(03)00059-2.

7. Nogueira, R.O. (2018). Analysis of the influence of lubrication with solid particles on the stamping of ABNT 1010 and 1020 steels. (Master's Thesis). Federal University of São João del Rei, Minas Gerais, Brazil.
8. Celestino, V. R. (2015). Comparative analysis of the use of uncoated hard metal tools coated with titanium diborete in wood machining. (Master's Thesis). Paulista State University, São Paulo, Brazil.
9. Chemical analysis by optical spectrometry (2021, 03 09). Retrieved from: https://www.labteste.com.br/analise-quimica-espectrometria.
10. Interchangeable cutting inserts (2021, 01 30). Retrieved from: https://www.dormerpramet.com/pt-pt/products/turning/turning?country=br.
11. Geometric product specifications (GPS) - Roughness (NBR ISO 4287). (2002). Rio de Janeiro, Brazil.
12. Indication of the state of surfaces in technical drawings – Procedure (NBR ISO 8404). (1984), Rio de Janeiro, Brazil.
13. Muhl, R.T. (2019). Optimization of finishing machining parameters through surface roughness in the turning of ABNT 4340 steel. (Master's Thesis). University of Passo Fundo, Rio Grande do Sul, Brazil.
14. Machado, A. R., & da Silva, M.B. (2009). Machining of metals. (Undergraduate Course) Federal University of Uberlândia, Minas Gerais, Brazil.
15. Xiao, Z., Liao, X., & Long, Z. (2017). Effect of cutting parameters on surface roughness using orthogonal array in hard turning of AISI 1045 steel with YT5 tool. International Journal Adv Manufacture Technology, p. 273–282, doi: 10.1007/S00170-016-8933-5.
16. Trent e. M., & Wright p. K. (2000). Metal cutting. Boston, EUA.
17. Kumar, A., Singh, A.K., & Singh, R.C. (2014). Review of effect of tool geometry variation on finish turning and improving cutting tool life. International Conference of Adance Research and Innovation: Department of Mechanical Engineering. Delhi, India, p. 566-571, doi: 10.1243/095440506X78192.

This page is intentionally left blank

Smart Surveillance System using Deep Learning

Dayana R, Suganya M, Balaji P, Mohamed Thahir A & Arunkumar P

ABSTRACT

In industry and research area big data applications are consuming most of the spaces. Among some examples of big data, the video streams from CCTV cameras as equal importance with other sources like medical data, social media data. Based on the security purpose CCTV cameras are implemented in all places where security having much importance. Security can be defined in different ways like theft identification, violence detection etc. In most of the highly secured areas security plays a major role in a real time environment. This paper discusses the detecting and recognising the facial features of the persons using deep learning concepts. This paper includes deep learning concepts starts from object detection, action detection and identification. The issues recognized in existing methods are identified and summarized.

Keywords: surveillance, security, real time, deep learning, face detection, face recognition.

Classification: FOR Code: 091599

Language: English

LJP Copyright ID: 392944
Print ISSN: 2631-8474
Online ISSN: 2631-8482

London Journal of Engineering Research

Volume 22 | Issue 3 | Compilation 1.0

Smart Surveillance System using Deep Learning

Dayana R[α], Suganya M[σ], Balaji P[ρ], Mohamed Thahir A[ω] & Arunkumar P[¥]

ABSTRACT

In industry and research area big data applications are consuming most of the spaces. Among some examples of big data, the video streams from CCTV cameras as equal importance with other sources like medical data, social media data. Based on the security purpose CCTV cameras are implemented in all places where security having much importance.

Security can be defined in different ways like theft identification, violence detection etc. In most of the highly secured areas security plays a major role in a real time environment. This paper discusses the detecting and recognising the facial features of the persons using deep learning concepts. This paper includes deep learning concepts starts from object detection, action detection and identification. The issues recognized in existing methods are identified and summarized.

Keywords: surveillance, security, real time, deep learning, face detection, face recognition.

I. INTRODUCTION

Now a day, securing highly Confidential matter from a third party is a challenging one. In recent times, accessing data from highly secured area had increased in number, so securing the data is essential. Most of the memory spaces of industry are occupied by the big data. The implementation of CCTV cameras in all areas due to security purpose. The use of CCTV cameras is essential, but it consumes more memory spaces to store data. Security is used for the purpose of theft identification, violence detection, unauthorized person entering, illegal activity in a region. Hence for all abnormal activity's security plays a major role so security must be implemented in the region of highly confidential. Using CCTV footage is past days methodology to find the theft happenings and other activities, this is a tedious process and time consuming. To overcome this existing methodology, CCTV camera is used with deep learning concepts for more ease. Deep learning concepts are capable of learning data which is unstructured, and it handles large amount of data sets. Deep learning will train the data sets and gives a finite data sets as a output. Using this concept training enormous amount of data as input and gives equal accurate data sets as an output. The accuracy rate is also a desirable one. Using deep learning, facial features of data sets are recognized with the help of CCTV. By this way all the data sets that are capturing in CCTV camera will be recognized and sort out the authorized person or unauthorized person as well. The video starts to record when there is an abnormal event has been recognized. This paper will summarize the drawback of existing technology over surveillance systems.

II. MOTIVATION

Security is essential where there is a more secured data. To secure large amount of data or highly securable data in confidential region security plays a major role. For establishing security for a data, it must be protected from an unauthorized person. The CCTV will capture the video and deep learning concepts will provide the features of facial analysis. When facial features are recognized it must be validated with authorized data sets in a database. The validated face is examined to find whether it is an authorized person or not. This concept will reduce the theft happening in real world areas and the person who attempt to enter the area in a unproper manner will be notified and caught. This paper reduces the theft happening or unauthorized way of entering.

London Journal of Engineering Research

2.1 Scope

The scope of this project is to minimize the theft happening in future and maximize the protection of a data in highly confidential region. This will be more essential in industry areas.

2.2 Objective

1. This will minimize the theft happening.
2. The administrator will be notified at the time of theft happening.
3. The data will be protected with high security in the confidential region.
4. The administrator will be notified regarding the abnormal activity in his/her place by a means of short message service or mail system using pop3 configuration.
5. The process is fast and highly securable.
6. This will summarize the past methodology and help to serve better for future purpose.

III. METHODOLOGY

The methodology design is based on **"Facial analysis and recognition".** In this paper we are describing about how security is established in an area having highly confidential data's and entering the prohibited area will be monitored without human. The security can be established by a means of deep learning concepts. With the use of deep learning techniques, security can be established by [1] facial detection [2] facial recognition [3] intimation. A major milestone within the development of automatic face recognition techniques was achieved by the introduction of extremely correct deep learning strategies like Deep face and Deep ID. For the primary time, face verification in free settings was achieved with accuracy surpassing human ability.

This development was solely allowed for by the appearance of great improvements in hardware, like high capability GPUs. Since then, the bulk of analysis has focused on the event of deep learning-based strategies that conceive to model the human brain, via high-level abstraction achieved employing a concurrence of non-linear filters leading to feature unchangeableness. the bulk of those strategies deem more and more deep CNNs, with an emphasis on promoting scantiness and property.

IV. RELATED WORKS

Facial recognition and verification are a region of high analysis interest because of its broad span of applications, the accessible scope for improvement in accuracy and process speed because of innovation in hardware and more and more massive and accessible databases. consequently, literature reviews are conducted sporadically to hide these changes. However, because of the large vary of face recognition ways utilized, most reviews specialize in a specific issue or set of issues, rather than addressing the complete vary of dominant ways. for instance, many recent surveys have specifically addressed a variety of methodologies that have tried to attain rotation. Other publications have reviewed face recognition techniques from numerous views. However, these surveys lack a comprehensive coverage of all presently relevant identity verification methodologies, and infrequently don't see the foremost current databases and benchmarks, like the Mega Face Challenge benchmark.

V. DATABASE

All identity verification and detection systems need the use face datasets for coaching and testing functions. In the accuracy of CNNs is extremely captivated with large coaching datasets. For example, the development of terribly giant datasets like Image Net, which contains over fourteen million pictures, has allowed the event of correct deep learning object detection systems. A lot of specifically, face detection and recognition datasets developed alongside benchmarks like the Mega Face Challenge[Fig 1.1]

Fig 1.1: Sample subset of mega face challenge dataset

The Face Detection Dataset and Benchmark (FDDB) dataset and the labelled Faces within the

Wild (LFW) dataset offer a way to check and rank face detection, verification and recognition systems, extremely difficult pictures in free settings. Notable and wide used datasets area unit in conjunction with info concerning their meant usage, size and the range of identities they contain. Upon analysis of the results earned by face verification and identification algorithms tested on small datasets like the LFW dataset, one is also LED to believe there remains very little scope for improvement. Once tested on sample pictures, algorithms achieving impressive results on smaller testing sets manufacture off from ideal accuracies as shown in [Fig1.2]

Fig 1.2: Different facial action of a training sets

The Mega Face Challenge was created in response to the saturation of tiny datasets and benchmarks, providing a large-scale public info and benchmark which needs all algorithms to be trained on the same information and tested on sample pictures, permitting honest comparison of algorithms while not the bias of personal dataset usage. However, despite the advantages bestowed by their size, each Mega Face challenge deprived by annotation problems and long tail distributions. The table1.1 shows the large collection of data sets for image processing.

Table 1.1: List of external sources contains large datasets

Database	Website	Features
Mega face	https://cs.nyu.edu/~roweis/data.html	3,000,000 images 572,000 identities
UMass data sets	http://vis-www.cs.umass.edu/lfw/	13,233 images 3,700 identities

VI. FACE DETECTION

Face detection may be a basic step in biometric authentication and verification. It additionally extends to a broad vary of alternative applications together with countenance recognition, face chase for surveillance functions, digital tagging on social media platforms and shopper applications in digital technologies, like auto-focusing ability in phone cameras. This survey can examine facial detection ways as applied to biometric authentication and verification. Historically, the best obstacle faced by face detection algorithms was the power to attain high accuracy in uncontrolled conditions. Consequently, their usability applications were restricted. However, since the face detection method, face detection settings has become commonplace. vital progress has since been created by researchers during this space thanks to the event of powerful feature extraction techniques. This review can or else target a lot of recently projected deep learning ways, that were developed in response to the restrictions and capturing salient facial info underneath at liberty conditions that embrace massive variations in resolution, illumination, pose, expression, and color. Essentially, it's the restrictions of those feature representations that have to date restricted the ability of classifiers to perform to the most effective of their ability.

Despite the increasing accuracy and speed of face detection systems, the 2 greatest challenges remain somewhat unresolved. Face detectors square measure needed to deal with giant and sophisticated variations in facial changes as shown in [Fig2.1], and effectively distinguish between faces and non-faces in unconstrained conditions. What is more, the big variation in face position and size at intervals an outsized search house presents challenges that cut back potency.

This requires a trade-off between high accuracy and procedure potency. One good thing about less correct Viola Jones galvanized cascade-based face detectors over CNN strategies is their potency. so, the best demand in the current field of analysis is that the development of additional economical CNN and Principal Component Analysis (PCA) face detection techniques. part addressed this issue, achieving the present state of the art accuracy rate of 88.5% on the arduous WIDER FACE take a look at set by developing the Face Attention Network (FAN), a novel face detector designed to boost recall in cases of occlusion while

not impacting on computation speed. This was achieved by exploitation associate anchor-level attention to reinforce facial features at intervals a face region, alongside random crop information augmentation to tackle occlusion and little faces.

Fig 2.1: Detecting facial features

VII. FATURE EXTRACTION

Feature extraction sometimes happens in real time once face detection and may be thought of together of the foremost vital stages in face recognition systems, as their effectiveness relies upon the quality of the extracted options. This can be as a result of facial landmarks and fiducial points known by a given network verify however accurately options are painted. Ancient fiducial purpose locators are model based, while several recent ways are cascaded regression based mostly.

Lately, key enhancements are created with the event of deep twin pathway ways, and other confidence map based mostly solutions.

Currently, the best defect gift within the realm of at liberty face alignment and fiducial purpose detection is that the lack of resolution to the matter of orienting faces no matter cause variation, and the general reliance of systems on correct face detection. The three hundred Faces within the wild info is mostly used for comparison of fiducial purpose detection ways. This face dataset is restricted, and therefore one space of improvement might embody the creation of a large scale annotated dataset containing a broad vary of at liberty facial pictures specifically designed to be used in face alignment and fiducial purpose detection applications. The facial features are extracted using PCA technique are shown in [fig3.1].

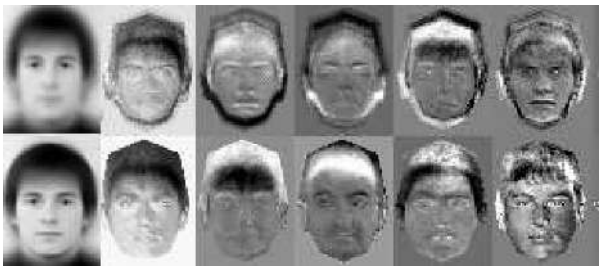

Fig 3.1: Feature extraction using PCA techniques

This might improve robustness across fiducial purpose detection usually, significantly with reference to cause and expression variations, low illumination and poor quality. With reference to network structures, deepening neural networks might capture a lot of abstract info which can assist in detection, however it's still unclear that network layers contribute most importantly to native options relevant to fiducial purpose detection. this is often one space which can enjoy more analysis. Furthermore, the high procedure value related to localizing fiducial points remains a significant challenge in at liberty conditions.

VIII. FACE IDENTIFICATION AND VERIFICATION

Subsequent to feature extraction, face recognition is performed. Recognition may be classified as either verification or identification. fashionable face recognition systems exploitation PCA involve deep feature extraction, and lastly, similarity comparison. A lot of specifically, verification

involves comparison of matched similarity between a groundwork image and a gallery of a far-famed identity, whilst identification determines one to several similarities to work out the identity of the probe. Both these processes need sturdy feature illustration, and a discriminative classification model.

The role of the loss perform is to work out the error within the prediction. totally different loss performs can output different error values for the same prediction, and therefore verify to an outsized extent the performance of the network.

Loss perform sort depends on the kind of downside, e.g. regression or classification. reduction of the error is achieved mistreatment back propagation of the error to a previous layer, whereby the weights and bias are changed.

Weights are learned and changed using Associate in Nursing improvement perform, like random gradient descent, that calculates the gradient of the loss perform regarding weights, then modifies weights to cut back the gradient of the loss function. The identification of data sets are shown in [fig 4.11] with accuracy value.

The sensitivity term is followed by decrease of the full error victimization the gradient descent methodology. This improves generalization and have extraction by shifting the neural activations of the hidden layers to the center high gradient space of the activation operate.

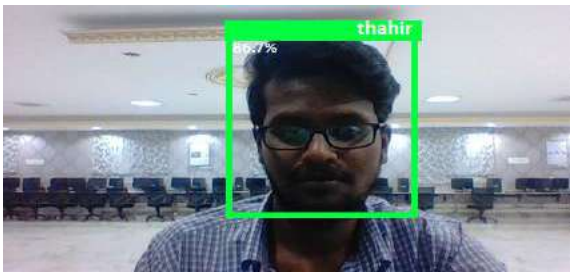

Fig 4.1: Identification of data set

IX. FUTURE SCOPE

In this project, we are using a smart surveillance camera to recognize the facial features of a person without his/her knowledge. This project will be more useful in industrial area and confidentiality sectors for right person to enter and access a highly secured matter.

X. RESULT AND CONCLUSION

This survey given an appraisal of recent face recognition methodologies, developments and challenges. It conjointly provided a comparative analysis of the obtainable databases, and connected benchmarks. It highlighted short-comings of state of the art strategies, and evaluated responses designed to deal with these limitations, accenting outstanding problems nevertheless to be addressed. Despite drastic enhancements in accuracy of illustration thanks to the non-linearity of deep feature representations, we can with confidence conclude that there's no famous ideal facial feature that's sufficiently sturdy for face recognition in free environments.

It should even be noted that solutions achieving state of the art accuracy are mostly inhibited by their dependence on sophisticated GPUs and huge databases, which means there's still adequate ought to focus analysis attention on a lot of ancient handcrafted feature representations.

Refinement of pruning strategies, and step-down of training time is additionally a neighborhood requiring attention, as is specification, which might profit from increased exiguity, and selectiveness. This project is very much useful to the industries and highly confidential areas. Due to high accuracy recognition only, the authorities can be allowed into the respective centers. This will reduce the effect of unauthorized person in confidential area.

REFERENCES

1. Y. Huang, Z. Liu, M. Jiang, X. Yu and X. Ding, "Cost-Effective Vehicle Type Recognition in Surveillance Images with Deep Active Learning and Web Data," in IEEE Transactions on Intelligent Transportation Systems, vol. 21, no. 1, pp. 79-86, Jan. 2020.
2. X. Geng, Z. Zhou and K. Smith-Miles, "Individual Stable Space: An Approach to Face Recognition Under Uncontrolled Conditions,"
3. Y. Shan, "ADAS and Video Surveillance Analytics System Using Deep Learning Algorithms on FPGA," 2018 28th International Conference on Field Programmable Logic and Applications (FPL), Dublin, 2018, pp. 465-4650.

London Journal of Engineering Research

4. L. Kang, I. Wang, K. Chou, S. Chen and C. Chang, "Image-Based Real-Time Fire Detection using Deep Learning with Data Augmentation for Vision-Based Surveillance Applications," 2019 16th IEEE International Conference on Advanced Video and Signal Based Surveillance (AVSS), Taipei, Taiwan, 2019, pp. 1-4.
5. M. V., V. V. R. and N. A., "A Deep Learning RCNN Approach for Vehicle Recognition in Traffic Surveillance System," 2019 International Conference on Communication and Signal Processing (ICCSP), Chennai, India, 2019, pp. 0157-0160.
6. J. Harikrishnan, A. Sudarsan, A. Sadashiv and R. A. S. Ajai, "Vision-Face Recognition Attendance Monitoring System for Surveillance using Deep Learning Technology and Computer Vision," 2019 International Conference on Vision Towards Emerging Trends in Communication and Networking (ViTECoN), Vellore, India, 2019, pp. 1-5.
7. J. Kim, Y. J. Mo, W. Lee and D. Nyang, "Dynamic Security-Level Maximization for Stabilized Parallel Deep Learning Architectures in Surveillance Applications," 2017 IEEE Symposium on Privacy-Aware Computing (PAC), Washington, DC, 2017, pp. 192-193.
8. G. Tourassi, "Deep learning enabled national cancer surveillance," 2017 IEEE International Conference on Big Data (Big Data), Boston, MA, 2017, pp. 3982-3983.
9. K. Muchtar, F. Rahman, M. R. Munggaran, A. P. J. Dwiyantoro, R. Dharmadi and I. Nugraha, "A unified smart surveillance system incorporating adaptive foreground extraction and deep learning-based classification," 2019 International Conference on Artificial Intelligence in Information and Communication (ICAIIC), Okinawa, Japan, 2019, pp. 302-305.
10. C. Xue, P. Liu and W. Liu, "Studies on a Video Surveillance System Designed for Deep Learning," 2019 IEEE International Conference on Imaging Systems and Techniques (IST), Abu Dhabi, United Arab Emirates, 2019, pp. 1-5.
11. R. Nayak, M. M. Behera, V. Girish, U. C. Pati and S. K. Das, "Deep Learning Based Loitering Detection System Using Multi-Camera Video Surveillance Network," 2019 IEEE International Symposium on Smart Electronic Systems (iSES) (Formerly iNiS), Rourkela, India, 2019, pp. 215-220.
12. K. Muchtar, F. Rahman, M. R. Munggaran, A. P. J. Dwiyantoro, R. Dharmadi and I. Nugraha, "A unified smart surveillance system incorporating adaptive foreground extraction and deep learning-based classification," 2019 International Conference on Artificial Intelligence in Information and Communication (ICAIIC), Okinawa, Japan, 2019, pp. 302-305.

Strain Energy Release Rate and Yield Strength for Normal and SCC with and without Glass and Steel Fibres

Swamy H. C. M & Prince Arul Raj G

ABSTRACT

Concrete is versatilely used building material. Its use in economical way is justified. Usually, torsion is predominant in water tank ring beam, canopy beams and cantilever retaining wall. Usually, failure in the structure is acceptable only after proper yielding of the material. According to limit state design philosophy balanced section is preferred. So here an attempt is made to identify yield strength of normal concrete and SCC with and without glass and steel fibres. Its torsional strain energy release is identified and in which concrete it is low and rate of taking the strength is discussed. Here plain concrete are considered. The performance is measured with respect to energy release and yield strength.

Keywords: strain energy release, yield strength, torsional strain energy.

Classification: DDC Code: 620.112 LCC Code: TA407.4

Language: English

London Journals Press

LJP Copyright ID: 392945
Print ISSN: 2631-8474
Online ISSN: 2631-8482

London Journal of Engineering Research

Volume 22 | Issue 3 | Compilation 1.0

Strain Energy Release Rate and Yield Strength for Normal and SCC with and without Glass and Steel Fibres

Swamy H. C. M[α] & Prince Arul Raj G[σ]

ABSTRACT

Concrete is versatilely used building material. Its use in economical way is justified. Usually, torsion is predominant in water tank ring beam, canopy beams and cantilever retaining wall. Usually, failure in the structure is acceptable only after proper yielding of the material. According to limit state design philosophy balanced section is preferred. So here an attempt is made to identify yield strength of normal concrete and SCC with and without glass and steel fibres. Its torsional strain energy release is identified and in which concrete it is low and rate of taking the strength is discussed. Here plain concrete are considered. The performance is measured with respect to energy release and yield strength.

Keywords: strain energy release, yield strength, torsional strain energy.

Author α: Part time research scholar at Karunya Institute of Science and Technology, Coimbatore, Tamil Nadu.
σ: Professor and Dean at Karunya Institute of science and Technology, Coimbatore, Tamil Nadu.

I. INTRODUCTION

Concrete and its use as a building material is well known fact. Its design, construction and maintenance are well justified. Before designing a structure, we have to select proper building material for its construction. Its behaviour under different loading condition has to be studied and the proper design philosophy has been selected and strength, serviceability and form should be satisfied. Here an attempt has been made to evolve a simple method to test a beam specimen subjected to torsion. Its strain energy is calculated and its rate of taking strain energy is evaluated for normal and self-compacted concrete with and with out glass and steel fibre is conducted.

As we know we have three design philosophy namely working stress, ultimate method and limit state method. In the limit state method, the strength and its serviceability are justified. The study on torsional strength is limited because it is included in compression, tension, flexure and shear. But here an attempt is made to study torsional behaviour completely by using fracture mechanics.

Fracture mechanics especially post fracture behaviour talks about material property and type of fracture either brittle fracture or elastic fracture. Fracture mechanics distinguish between brittle and other than brittle fracture. Linear elastic fracture mechanics (LEFM) talks about the difference between brittle fracture and elastic fracture.

The material toughness at the on set of fracture at plane-strain is denoted by $K_{IC.}$ The plain -Strain K_{IC} is based on the lowest load at which crack occurs. Strain energy release rate at fracture is given by G_{IC} and its relation ship with K_{IC} is related as follows:

$G_{IC} = K^2_{IC} / E$ --------- For Plane Stress
$G_{IC} = K^2_{IC} / (E (1-V^2))$---- For Plane strain
E = Modulus of elasticity of concrete
V = Poisson ratio

II. LITERATURE REVIEW

Application of fracture mechanics to study the improved behaviour of concrete under tensile loads was first adopted by Romualdi and Baston. Griffith suggest that the fracture of a brittle material is due to the presence of small cracks and proposed a theory of fracture strength based on the changes in the strain energy and surface energy as the crack extends. The Griffith approach

was extended to ductile material by Orowan[3] and Irwin. The strain energy release rate which Irwin denoted by G_{IC} , may generally, be less than that is required to cause unstable crack propagation. The strain energy release rate at the on set of the unstable crack propagation was referred to as the critical strain-energy release rate G_{IC}. G_{IC} is regarded as a material property where as G_{IC} is primarily a function of loading and geometry of the system.

Not much work is conducted on, to relate the yield strength and strain energy release rate. A simple procedure with relating the material property and load has been established in this work.

Objectives of the study

1. To evaluate Yield strength for normal and SCC with and without glass and steel fibres.
2. To calculate strain energy release rate for plane stress and plane strain conditions.
3. To discuss the material property based on yield strength criteria.
4. To develop the relation between Youngs modulus and yield strength.
5. To develop the poisons ratio relation with strain energy release rate.
6. To explain failure criteria of the material for normal and SCC with and with out glass and steel fibres.
7. To explain how the fibres and microstructures behaviour for the torsional strain energy.
8. Compare the normal concrete, SCC and its behaviour with and with out glass and steel fibres.

Experimental Set Up and Procedure

Fig 1: Showing the Torsional Strain Energy Experiment in KIT lab

The experimental set up to conduct the torsional strain energy is shown in the above Fig 1. and the procedure for testing and conducting the experiments are listed in the table 1. below. The Concrete considered for the test is M30 and cement used is ACC and Chemicals used is AS chemicals with silica fume as mineral admixture.

Table 1: Experimental Details

Name of Experiment	Total Number of Specimens	Remarks
Slump Cone Test	51	Free fall
Spread Test	51	Free flow
V- Funnel - Test	51	Time in Sec
L-Box Test	51	Ratio
Compression Test	51 Cubes 150 x 150 x150 mm	Strength
Split Tensile Strength	51 Cylinders 150 mm Diameter and 300mm height	Tensile strength
Concrete Mix Design	154 Cubes 150 x 150 x 150 mm	Characteristic Strength
Flexural Strength	51 beams of 100 x 100 x 500 mm	Two-point Bending Test Load- deflection
Torsional Strength	51 beams of 100 x 100 x 500 mm	Measurement of Torque
Total No of Specimen Tested	562	

Experimental Results:

Table 2: Values of Density for ordinary concrete and SCC with and without GF and SF

Type of Concrete	Density Experimental Kg/m^3
Normal Concrete	2292
SCC (S.P-0.5%)	2150
SCC (S.P-1.0%)	2230
SCC (SP-1.50%)	2169
SCC (SP-2.0%)	2050
SCC (SP-0.5%, GF-0.2%)	2166
SCC (SP-0.1%, GF-0.4%)	2150
SCC (SP-1.5%, GF-0.8%)	2128
SCC (SP-2%, GF-1%)	2342
Normal Concrete (S.P-0.5%, GF-0.2%)	2150
Normal Concrete (S.P-1.0%, GF-0.4%)	2339
Normal Concrete (S.P-1.5%, GF-0.8%)	2158
Normal Concrete (S.P-2.0%, GF-1%)	2087
SCC (SP-0.5%, SF-0.2%)	2150
SCC (SP-1.0%, SF-0.4%)	2128
SCC (SP-1.5%, SF-0.8%)	2342
SCC (SP-2.0%, SF-1.0%)	2303

Table 3: Values of Youngs Modulus (E)for Different Types of M30 Concrete. Theoretical Value of E = 27386MPa

Type of Concrete	Youngs Modulus Experimental
Normal Concrete	34800 MPa
SCC (S.P-0.5%)	20616MPa
SCC (S.P-1.0%)	26458MPa
SCC (SP-1.50%)	28285MPa
SCC (SP-2.0%)	22913MPa
SCC (SP-0.5%, GF-0.2%)	264397MPa
SCC (SP-0.1%, GF-0.4%)	24036MPa
SCC (SP-1.5%, GF-0.8%)	21131 MPa
SCC (SP-2%, GF-1%)	92600 MPa
Normal Concrete (S.P-0.5%, GF-0.2%)	25778 MPa
Normal Concrete (S.P-1.0%, GF-0.4%)	26665 MPa
Normal Concrete (S.P-1.5%, GF-0.8%)	20869 MPa
Normal Concrete (S.P-2.0%, GF-1%)	19033 MPa
SCC (SP-0.5%, SF-0.2%)	27514 MPa
SCC (SP-1.0%, SF-0.4%)	25691 MPa
SCC (SP-1.5%, SF-0.8%)	23717 MPa
SCC (SP-2.0%, SF-1.0%)	20494 MPa

Table 4: Strain Energy Release Rate (G_{IC}) and Yield Strength

Type of Concrete	Yield Strength MPa	G_{IC} – Plane Stress MPa	G_{IC} – Plane strain_ MPa_
Normal Concrete	40.44	6.942×10^{-9}	7.15×10^{-9}
SCC (S.P-0.5%)	46.154	3.9×10^{-9}	4.03×10^{-9}
SCC (S.P-1%)	56.73	1.26×10^{-8}	1.29×10^{-8}
SCC (S.P-1.5%)	52.91	4.20×10^{-9}	4.30×10^{-9}
SCC (S.P-2%)	45.71	5.644×10^{-8}	5.77×10^{-8}
SCC (SP-0.5%, GF-0.2%)	48.09	2.62×10^{-8}	2.68×10^{-8}
SCC (SP-1%, GF-0.4%)	52.87	5.57×10^{-8}	5.70×10^{-8}
SCC (SP-1.5%, GF-0.8%)	42.06	4.59×10^{-9}	4.60×10^{-9}
SCC (SP-2%, GF-1%)	18.56	1.02×10^{-8}	1.04×10^{-8}
Normal Concrete (SP-0.5%, GF-0.2%)	51.59	3.78×10^{-8}	3.87×10^{-8}
Normal Concrete (SP-1%, GF-0.4%)	53.33	1.06×10^{-6}	1.10×10^{-7}
Normal Concrete (SP-1.5%, GF-0.8%)	41.74	6.79×10^{-9}	6.94×10^{-9}
Normal Concrete (SP-2%, GF-1%)	38.15	8.43×10^{-7}	1.39×10^{-8}
SCC (SP-0.5%, SF-0.2%)	51.39	2.07×10^{-8}	1.93×10^{-8}
SCC (SP-1%, SF-0.4%)	55.03	8.81×10^{-7}	1.63×10^{-8}
SCC (SP-1.5%, SF-0.8%)	47.54	7.52×10^{-9}	7.72×10^{-9}
SCC (SP-2%, SF-1%)	40.96	9.34×10^{-9}	9.56×10^{-9}

III. DISCUSSIONS

Yield strength of SCC with super plasticizer dosage of 1% is having maximum value of 56.73(Table-3) indicating that the super plasticiser improves the workability at normal W/C ratio of 0.4. The mix also gives an idea that the micro structure contains less pores and developed good gel -pores which filled the pores and making concrete more attaining ultimate strength before fracture. This mix is costly because super plasticiser dosage is 1% and the industry permits 0.5% as maximum dosage for big works.

Similarly, with the normal concrete with super plasticizer 1% and Glass fibre 0.4% (Table1) which is the mix which is economical and gives maximum yield strength. This mix having good strain energy release rate and we can recommend it as design mix. The density (Table2) and modulus of elasticity of the mix is dominating comparing with the other mixes. So, from the (Table 3) gives that it is having good modulus of elasticity. The glass fibre is having good modulus of elasticity and ultimate strength compared to steel fibres. The reason for its good property is that it develops good bond between the aggregate phase, cement mortar phase and interfacial transition zone. The applied load creates a system in this matrix in such a mode that the yield strength and E values and its density giving a good torsional strain energy release value.

The poisons ratio for strength can be taken as 0.15 and for serviceability it is 0.2. The yield strength, modulus of elasticity and strain energy release rate all are maximum in normal concrete with 0.4% glass fibres with 1% super plasticizer. This mix in this paper is the deciding mix . Even other mixes may give little high or low values of yield strength, modulus of elasticity and torsional strain energy release.

The failure criteria indicates that the strain energy release which is having good yield strength and at plane strain or plane stress condition is considered, it is elastic plastic failure. The material which is having glass fibre with good super plasticizer gives good strength and serviceability conditions. The normal concrete mix with fibres gives good yield strength and strain energy release rate.

The material behaviour is different at different loading conditions and here we are evaluating a very sensitive term torsional strain energy which describes the material property at microscopic level. The study of the concrete with different types of fibres with different dosages for normal and SCC gives a clear idea about the physical, mechanical and microstructural behaviour of concrete.

mechanical and microstructural behaviour of concrete.

Conclusions and remarks

Torsional strain energy release and yield strength criteria gives two types of material property evaluation and checking the micro structure of concrete mechanically. This work clearly indicates thar the modulus of elasticity, density, yield strength and strain energy release are maximum for normal concrete with 0.4% glass fibres and 1% super plasticizer gives very good result. But by decreasing the dosage of superplasticizer indicates that the workability decreases and requires high W/C ratio which reduces the strength drastically.

SCC can be used with different dosages of superplasticizer and fibres with proper mix design criteria.

REFERENCES

1. Romualdi J.P. and Batson G.B.," Mechanics of crack arrest in concrete," Journal of Engg Mechanics Division Proceedings, ASCE, Vol. 89, EM 3, June 1963,pp.147-160
2. Romualdi, J.P. and Batson, G.B.,'Behaviour of reinforced cement concrete beams with closely spaced reinforcement', Journal of the American Concrete Institute, Proceedings Vol.60, No.6, June 1963, pp.775-789.
3. Romualdi, J.P. and Mandel,J.A.,"Tensile strength of concrete affected by uniformly distributed and closely spaced short lengths of wire reinforcement',Journal of the American Concrete Institute, Proceedigs, Vol.61,No.6, June 1964, pp.657-670
4. Shah, S.P. and Rangan, B.V.,'Effects of reinforcements on ductility of concrete', Journal of the Structural Division Proc.,ASCE, Vol,96,ST 6. June 1970,pp.1167-1184
5. Rajagopalan, K. Parameswaran, V.S. and Ramaswamy, G.S.,"Strength of steel fibre reinforced concrete beam", The Indian concrete Journal, Vol. 48, No.1, Jan 1974,pp.17-25
6. Pakotiparapha, B,. Pama, R.P. and Lee, S.L,"Mechanical properties of cement mortar with randomly oriented short steel wires" Magazine of Concrete Research, Vol.26, No.86, March 1974,pp.3-15
7. Tattersall, G.H. and Urbanowicz, C.R.,"Bond strength in steel fibre reinforced concrete', Magazine of concrete research, Vol.26, No.87, June 1974,pp.105-113
8. Kar.J.N. and Pal.AK,"Strength of fibre reinforced concrete", Journal of the Structural Division, Proc.ASCE, Vol.98,(ST-5), May 1972 pp-1053-1068
9. Ramey, M.R.,"Compression fatigue of fibre reinforced concrete", Journal of Engineering Mechanics Division, ASCE, Vol.100, EM 2, April 1974, pp.139-149
10. Shah, S.P. and Vijayarangan, B., "Fibre reinforced concrete properties", Journal of American Concrete Institute Proceeding Vol.68. No.2. Feb 1971, pp.126-135
11. Chen, Klal-Fah and Carson, J.L.,"Stress-Strain properties of random wire reinforced concrete", Journal of American Concrete Institute, Proceedings Vol.68, No, Dec1971. pp-933-936.
12. Snyder, M.J and Lankard, D.R. "Factors affecting the flexural strength of steel fibrous concrete", Journal of American Concrete Institute, Proceedings Vol.69, No2, Feb 1972 pp-96-100
13. "Fibre Reinforced Concrete", Proceedings of the International Symposium Ottawa, oct 1973 publication of ACI, SP-44,1974,pp.554
14. Krishna Raju, N. et al., "Compressive Strength and Bearing Strength of steel fibre reinforced concrete", Indian Concrete Journal, Vol.51, No.6, June 1977,pp.103-108

This page is intentionally left blank

Simulation Study of Lead Removal from WasteWater by using Tea Waste as Biosorbent

Thavaambigai Revichandran & Nurul Huda Binti Baharuddin

Universiti Teknologi Malaysia

ABSTRACT

Toxic heavy metals such as lead have been discharged into water streams due to industrialization, particularly from the stationery industry. Even though there are several ways to remove heavy metals, running the procedures is quite expensive. As a result, this research will simulate the performance of tea waste as a bio sorbent agent for removing lead ions from wastewater. The Fixed-Bed Adsorption Simulation Tool (FAST) program will create a simulation in this investigation. Furthermore, different manipulation factors such as lead ion initial concentration, contact time, and adsorbent dose were employed to evaluate its influence on the biosorption process. The results are comparable to a previous study on tea waste as a source of biosorption. According to the previous research and case study, the optimal contact duration is 60 minutes, the best metal ion concentration for adsorption is 100 mg/L, and the best adsorbent dose is 2 g. Furthermore, a comparison of the Langmuir isotherm with the Freundlich isotherm reveals that the Langmuir isotherm produces better results. Moreover, when the pseudo-first-order kinetic model is compared to the pseudo-second-order kinetic model, the pseudo-first-order yields superior results.

Keywords: tea waste, FAST, simulation, lead ions.

Classification: DDC Code: 394.15 LCC Code: GT2910

Language: English

London Journals Press

LJP Copyright ID: 392946
Print ISSN: 2631-8474
Online ISSN: 2631-8482

London Journal of Engineering Research

Volume 22 | Issue 3 | Compilation 1.0

Simulation Study of Lead Removal from WasteWater by using Tea Waste as Biosorbent

Thavaambigai Revichandran[α] & Nurul Huda Binti Baharuddin[σ]

ABSTRACT

Toxic heavy metals such as lead have been discharged into water streams due to industrialization, particularly from the stationery industry. Even though there are several ways to remove heavy metals, running the procedures is quite expensive. As a result, this research will simulate the performance of tea waste as a bio sorbent agent for removing lead ions from wastewater. The Fixed-Bed Adsorption Simulation Tool (FAST) program will create a simulation in this investigation. Furthermore, different manipulation factors such as lead ion initial concentration, contact time, and adsorbent dose were employed to evaluate its influence on the biosorption process. The results are comparable to a previous study on tea waste as a source of biosorption. According to the previous research and case study, the optimal contact duration is 60 minutes, the best metal ion concentration for adsorption is 100 mg/L, and the best adsorbent dose is 2 g. Furthermore, a comparison of the Langmuir isotherm with the Freundlich isotherm reveals that the Langmuir isotherm produces better results. Moreover, when the pseudo-first-order kinetic model is compared to the pseudo-second-order kinetic model, the pseudo-first-order yields superior results.

Keywords: tea waste, FAST, simulation, lead ions.

Author α: School of Chemical and Energy Engineering, Faculty of Engineering, Universiti Teknologi Malaysia, 81310 UTM Johor Bahru, Malaysia.

I. INTRODUCTION

Lead was among the first elements that mankind encountered, and it was utilised as early as 3000 B.C. Lead was used to create pipework and bath linings by the ancient Romans, and the plumber who joins and repairs pipes derives his name from the Latin term plumbum, meaning lead. Plumbum is also the name of the surveying phrases "plumb bob" and "plumb line," as well as the chemical symbol for lead, Pb [1]. Although it can exist in numerous chemical forms, Pb does not disintegrate in the environment. Pb-containing particulate particles can travel through the air, water, and soil. In general, atmospheric deposition is the most common source of Pb in soils that are not influenced by other non-air sources (e.g., dust from deteriorating leaded paint) [26].

The WHO's method for assessing the global burden of illness is DALYS or disability-adjusted life years; they are defined as the total of years of life lost due to death and impairment due to a certain illness or condition case, lead exposure [19]. The entire disease burden due to lead is estimated to be over 9 million DALYs (disability-adjusted life years)! This DALY estimate is mostly due to mental impairment (as assessed by IQ), but it also includes elevated blood pressure (which raises the risk of ischemic heart disease), stroke, hypertensive illness, and other cardiovascular illnesses (WHO). In addition, lead poisoning was predicted to be responsible for 143,000 fatalities and 0.6 percent of the worldwide disease burden in 2004 [22].

Besides, biosorption is an effective and environmental-friendly method to treat wastewater. Metal biosorption is used to remove metal ions from aqueous streams using agricultural products [21]. A solid phase (sorbent) and a liquid phase (solvent) containing a dissolved species to be sorbed are involved in the biosorption process. Due to the sorbent's high affinity for metal ion species, the latter is attracted and bound by a complicated process comprising chemisorption, complexation, adsorption on surface and pores, ion exchange, chelation, and physical force adsorption.

There are a variety of biomaterials with different sorption capabilities. The utilisation of these materials is based on their sorption capacity as well as their reusability over time [11]. Hence, tea waste will be employed as a bio sorbent in this investigation to aid lead biosorption. Tea comes in various flavours, including green, black, and Oolong; all tea drinks are made from the same fundamental tea leaves (Camellia sinensis L.). Extracts from it are utilised in various drinks, health foods, nutritional supplements, and cosmetic products [10].

Furthermore, FAST is an acronym for Fixed-bed Adsorption Simulation Tool. FAST is a water treatment program that predicts the breakthrough curves of fixed-bed adsorption filters by the simulation method. [25] Various adsorbent media, such as granular activated carbon (GAC) or metal oxides, can be used depending on the pollutant to be removed in the process. Determining kinetic parameters from laboratory tests is another use. The homogeneous surface diffusion model (HSDM) and the linear-driving force approximation may both be solved numerically with FAST (LDF). are a valuable teaching tool for water engineering and water chemistry classes because of the extensive built-in support. [25]

II. METHODOLOGY

As previously indicated, we will compare the simulation findings to the experimental data in this simulation research. As a consequence, the experimental result from Mehrdad Cheraghi's publication "Removal of Pb (II) from Aqueous Solutions Using Waste Tea Leaves" is being compared to our simulation of Lead (Pb II ion) removal using tea waste.

Furthermore, the categorization of bio-sorbent properties is regarded as the initial technique here. Table 3 shows the characteristics of tea waste used by the experimental research, which will also be used in this simulation study.

Table 2.1: The characteristics of tea waste for this simulation study

Parameter	Tea Waste Values
Humid (%)	10.5
Density (g cm^{-3})	0.353
Dissolved material (%)	81
Solution particles total (mg 1^{-1})	108
Organic matters (%)	85
Ash content (%)	2.85
pH_{ZPC}	6

Many process factors such as contact duration, adsorbate concentration, and adsorbent dose were evaluated. Hence, several parameters are calculated and compared with the experimental research to obtain the values for the simulation to run. Firstly, the bed density was calculated using data from an experimental case study on Pb (II) biosorption by tea waste. The diffusion coefficient for the film is considered to be proportional to the surface area and the difference in concentration between the bulk solution and the adsorbent surface. k_L may also be calculated by fitting the simulation to experimental data. Besides, empirical correlations for the Sherwood number are used to calculate the film diffusion coefficient k_L.

$$\frac{\partial M}{\partial t} = k_L A(c - c^*) \quad (1)$$

$$A = \pi d_p^2 \quad (2)$$

Fick's second law is used to simulate mass transport in the adsorbent grain, which is considered to be homogeneous surface diffusion—fitting the simulation to experimental data yields the surface diffusion coefficient DS.

$$\frac{\partial q}{\partial t} = D_s\left(\frac{\partial^2 q}{\partial r^2} + \frac{2}{r}\frac{\partial q}{\partial r}\right) \quad (3)$$

To investigate the kinetics of Pb (II) adsorption by tea waste, 100 ml of 100 mg/L Pb (II) solution was mixed with known quantities of each adsorbent. For Pb, the program got to run for 120 minutes. The adsorption kinetics of Pb (II) ions were studied using Lagergren's pseudo-first-order kinetics expression and pseudo-second-order rate expression equation.

Table 2.2: The overall kinetic models used in this study

Reaction Kinetic Models	Non-Linear Equation	Linear Equation	Model Parameters
pseudo-first order	$q_t=q_e\ (1-e^{-k1t})$	$log(q_e - q_t) = logq_e - (\frac{k_1}{2.30}$	q_e, k_1
pseudo-second order	$q_t= q_e^2k_2t/(1+q_ek_2t)$	$\frac{t}{q_t} = \frac{1}{k_2q_e^2} + \frac{t}{q_e}$	q_e, k_2

The adsorption of Pb (II) ions by tea waste particles adsorbents was studied using two Langmuir and Freundlich adsorption isotherm models. [18]

The Langmuir isotherm model can be written as follows:

$$q_e = \frac{Q_m K_L C_e}{1+ K_L C_e} \tag{4}$$

Where:

q_e = the amount of lead adsorbed equilibrium (mg/g)

Q_m = the maximum monolayer coverage capacity (mg/g)

K_L = the Langmuir isotherm constant (L/mg)

The Freundlich Isotherm can be identified through:

$$logq_e = logk_F + \frac{1}{n} logC_e \tag{5}$$

Where:

C_e = The Lead ion's equilibrium concentration in the remaining solution (in mol/L)

q_e = The adsorbed Lead ion's equilibrium concentration per unit of mass sorbent (in mol/g)

k_F = The capacity for adsorption

n = Related to the adsorption intensity (unitless)

To study the effect of contact time, the contact time is varied in the range from 30 mins, 60 mins and 90 mins. The other parameters are being held constant for this study, like the Pb (II) ion concentration in wastewater to 100 mg/L and the mass of tea waste to 2g on each run. The effect of initial bio sorbent dose on % of Pb (II) ion elimination was investigated by adjusting the bio sorbent concentration of 1g, 2g and 3g. A graph of adsorption capacity vs contact time after 120 minutes was generated. To investigate the effect of metal ion concentration on the lead removal from the wastewater using the tea waste, the concentration of lead solution differs from 100 mg/L to 300 mg/L. The contact time is 60 min while the adsorbent dose is also kept constant to 2g for each run. To investigate the effect of metal ion concentration, the concentration of lead solution differs from 100 mg/L to 300 mg/L. The contact time is set to be as before which is 60 min while the adsorbent dose is also kept constant to 2g for each run.

III. RESULTS AND DISCUSSION

3.1 Comparison of Biosorption Isotherms with Experimental Study

In this case study, the Langmuir and Freundlich isotherms were investigated. The simulation was done using the identical settings (2g adsorbent mass, 100mg/L Pb(II) concentration, 60 minutes contact duration) for both isotherms. Figures 3.1 and 3.2 depict simulation runs for the Langmuir and Freundlich isotherms, respectively.

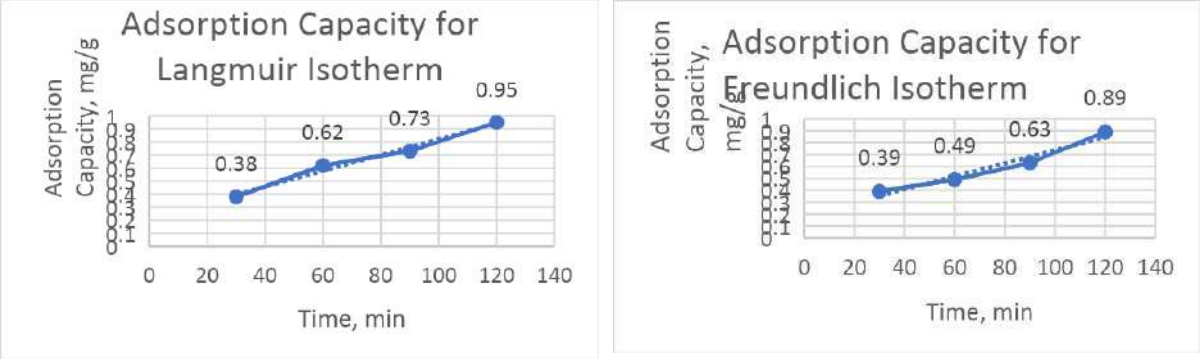

(a) (b)

Figure 3.1 a & 3.1 b: Simulation run for the adsorption capacity for Langmuir Isotherm and Freundlich Isotherm using FAST

According to Figures 3.1 and 3.2, the Langmuir isotherm has a higher R^2 value of 0.9823 than the Freundlich isotherm. Other research studies comparing Freundlich and Langmuir isotherms have also found that the Langmuir isotherm gives the greatest value of R^2 correlation, suggesting that it is the best fit model to forecast the data's trendline. Consequently, it may be inferred that the Langmuir isotherm outperforms the Freundlich isotherm. As a result, the same procedure of comparing R2 is utilised to determine the most accurate isotherm for this case study.

3.2 Kinetic Study on the Lead Removal

Both the pseudo-first-order and pseudo-second-order kinetic models were explored in this research. Both models were simulated using the same parameters (2g adsorbent mass, 100mg/L Pb (II) concentration, 60 minutes contact time). Simulation runs for the pseudo-first-order and pseudo-second-order kinetic models are shown in Figures 3.3a and 3.3b, respectively.

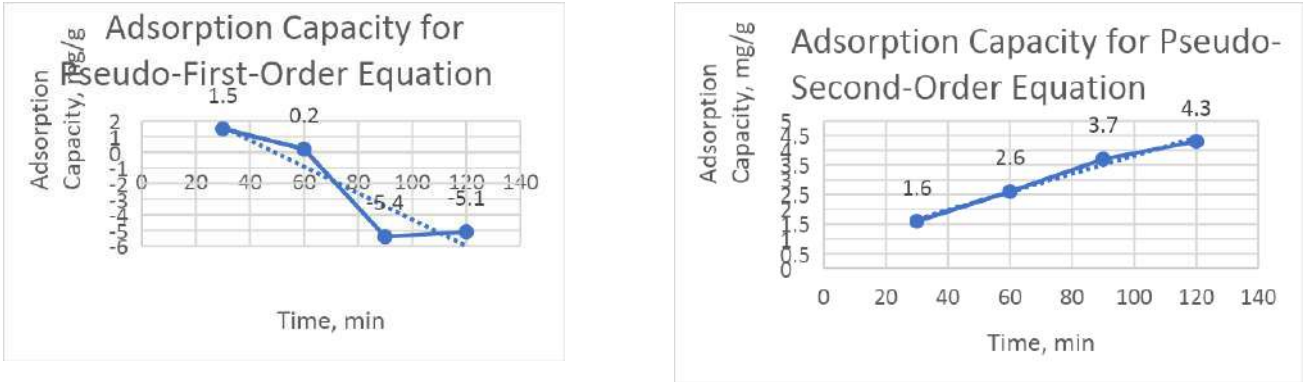

Figure 3.2a & 3.2b: Simulation run for Pseudo-first-order equation and Pseudo-second-order equation

The pseudo-second-order kinetic model has a higher and more suitable R^2 value than the pseudo-first-order kinetic model. Other studies that compared pseudo-first-order and pseudo-second-order kinetic models discovered that the pseudo-second-order model had the highest R^2

correlation, implying that it is the best-suited model for forecasting the data's trendline.

3.3 Comparison Study of Variables on Simulation Results with Experimental Results

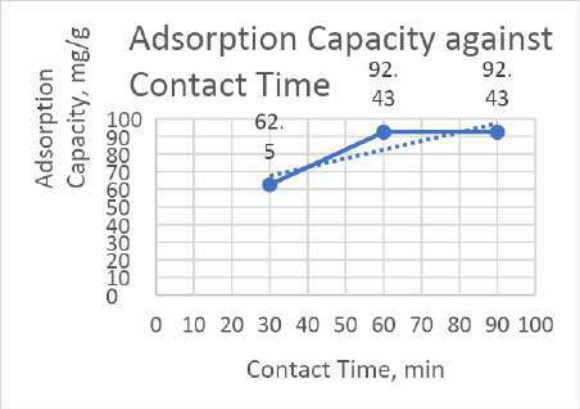

(a)

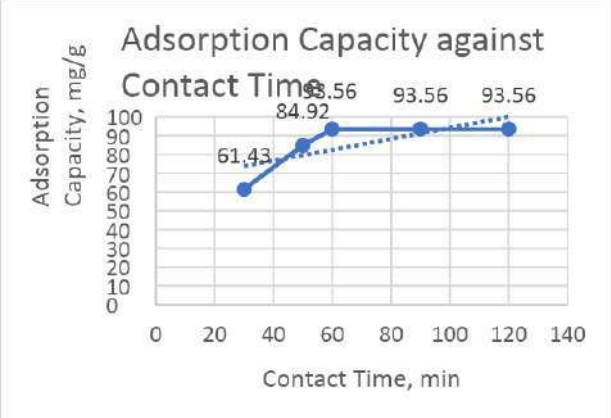

(b)

Figure 3.3 a & 3.3 b: Effect of contact time on the adsorption capacity of tea waste for simulation run and experimental research

Both the simulation and experimental values indicate a rising trend in adsorption capacity and then become static after a while, with little difference in the values. Moreover, both findings demonstrated that the best contact time for the maximum adsorption capacity of the tea waste particle occurs at the 60th minute. The adsorption rate was quick at the beginning of the contact period due to a large number of accessible adsorbent surfaces. The lower adsorption effectiveness over some time might be attributable to two factors. To begin with, occupying the sites limited the number of active surface sites available on the adsorbent. Second, owing to the repulsive effect of the deposited metal ions on the solid and bulk phase, the remaining unoccupied surface sites were difficult to occupy.

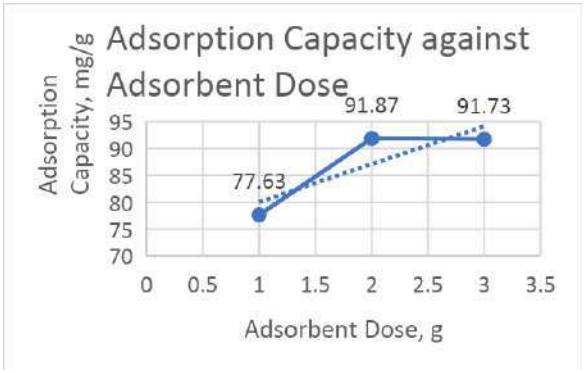

(a)

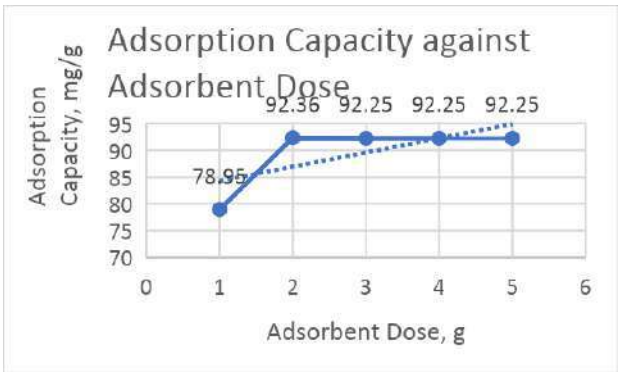

(b)

Figure 3.4 a & 3.4 b: Effect of adsorbent dose on the adsorption capacity of tea waste for simulation run and experimental research

Both simulation and experimental results show a growing trend in adsorption capacity and reduce with successive dose increments until becoming static beyond a specific dosage, with less variation in the result data. Adsorption of Pb (II) is expected to rise when the adsorbent dosage is increased. It was raising the adsorbent dosage gives more adsorption sites for a constant starting adsorbate concentration, the removal efficiency improves with increasing the adsorbent dose. Metal ion binding to tea waste's surface functional groups is another possible explanation. But beyond a certain point, increasing the amount did not influence removal effectiveness, and 2g was the optimum amount proven from both the experimental and simulation study. We discovered a similar behaviour with Zn (II) [23]. As a result, the adsorption capacity is influenced by the adsorbent mass.

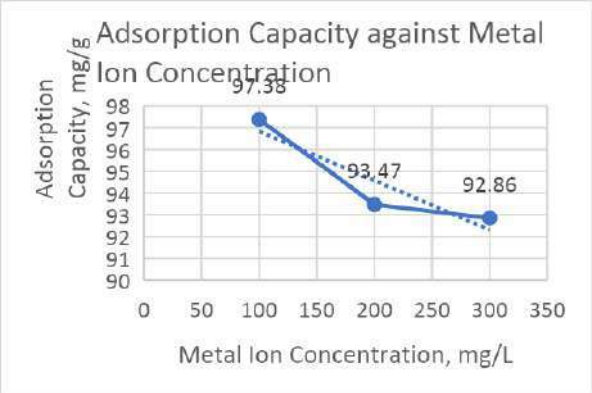

(a)

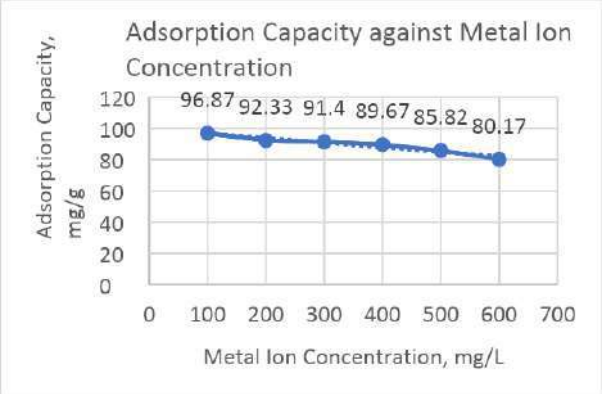

(b)

Figure 3.5 a & 3.5 b: Effect of metal ion concentration on the adsorption capacity of tea waste for simulation run and experimental research

As the metal ion concentration increases, the simulated and experimental values reveal a declining trend in adsorption capacity, and the value difference is not particularly noticeable. A rise in the initial Pb (II) concentration may have increased the driving power of the concentration gradient. As a result of the restricted number of active adsorbent particle sites and the limited uptake capacity, the removal efficiency is high at low concentrations. In contrast, when the metal concentration is high, the active sites of the adsorbent particles are occupied. Hence, it can be concluded that Pb (II) concentration will influence the adsorption capacity. Furthermore, both analyses revealed that the ideal metal ion concentration for achieving maximal adsorption capacity is 100 mg/L.

IV. CONCLUSION

In a nutshell, the effectiveness of tea waste as a bio-sorbent for lead ion adsorption in wastewater was investigated successfully. According to this case study, tea waste is an effective bio-sorbent for adsorbing lead in wastewater. It was found that ideal contact time for adsorption is 60 minutes. 100mg/L, 200mg/L, and 300mg/L of metal ion concentration were utilised in the investigation of Pb (II) concentration and adsorption capacity, and 100mg/L of metal ion concentration recorded the best adsorption capacity compared to other concentrations. The adsorbent doses employed in this case study were 1g, 2g, and 3g, with the 2g dosage having the best adsorption capacity. The comparison of Langmuir isotherm with Freundlich isotherm reveals that Langmuir isotherm outperforms Freundlich isotherm. Moreover, this study also proved that the pseudo-second-order kinetic model is the best fit model for this investigation compared to the pseudo-first-order kinetic model. Furthermore, in this case, study, the accuracy of the simulation data was determined. The adsorption process which was aided by the FAST program, gave accurate data. Because FAST software is specifically created to analyze adsorption processes, it was utilised in this case study to investigate the influence of contact time, metal ion concentration, and adsorbent dose on the adsorption capacity of tea waste particles in the removal of lead from the wastewater. As a result, FAST software is employed in this case study to evaluate its efficiency, and the results are favourable.

ACKNOWLEDGEMENTS

This research is fully supported by the UTM grant GUP Tier 2, PY/2019/00603-Q.J130000.2611 for funding along the way to accomplish this research work.

REFERENCES

1. Adsorptive Removal of Lead and Zinc Ions From Aqueous Solution using Thiolated Tea (Camellia sinensis) Seed Shell. (2015). Iranica Journal OF Energy & Environment, 6(3).
2. Ahluwalia, S. S., & Goyal, D. (2005). Removal of Heavy Metals by Waste Tea Leaves from Aqueous Solution. Engineering in Life Sciences, 5(2), 158–162.
3. Alwared, A. P. D. A., & Ali Sadiq, N. (2017). Competitive Removal of Lead Copper and Cadmium from Aqueous Solution onto Tea

Waste. Association of Arab Universities Journal of Engineering Sciences, 24(3), 43-62.
4. Amarasinghe, B., & Williams, R. (2007). Tea waste is a low-cost adsorbent for the removal of Cu and Pb from wastewater. Chemical Engineering Journal, 132(1–3), 299–309.
5. Anastopoulos, I., Pashalidis, I., Hosseini-Bandegharaei, A., Giannakoudakis, D. A., Robalds, A., Usman, M., Escudero, L. B., Zhou, Y., Colmenares, J. C., Núñez-Delgado, A., & Lima, D. C. (2019). Agricultural biomass/waste as adsorbents for toxic metal decontamination of aqueous solutions. Journal of Molecular Liquids, 295, 111684.
6. Cheraghi, M., & Sobhanardakani, S. (2015). Removal of Pb (II) from Aqueous Solutions Using Waste Tea Leaves. Iranian Journal of Toxicology, 9 (No 28).
7. Condon, J. B. (2006). Surface Area and Porosity Determinations by Physisorption: Measurements and Theory: Elsevier Science.
8. ELTurk, M., Abdullah, R., Zakaria, R. M., & Bakar, N. K. A. (2019). Heavy metal contamination in mangrove sediments in Klang estuary, Malaysia: Implication of risk assessment. Estuarine, Coastal and Shelf Science, 226.
9. Environmental Quality (Sewage and Industrial Eftluents) Regulations, (1979).
10. Garcia-Chevesich, P., García, V., Martínez, G., Zea, J., Ticona, J., Alejo, F., Vanneste, J., Acker, S., Vanzin, G., Malone, A., Smith, N. M., Bellona, C., & Sharp, J. O. (2020). Inexpensive Organic Materials and Their Applications towards Heavy Metal Attenuation in Waters from Southern Peru. Water, 12(10), 2948.
11. Guo, X., & Wang, J. (2019). A general kinetic model for adsorption: Theoretical analysis and modeling. Journal of Molecular Liquids, 288.
12. Hand, D. W., Crittenden, J. C., & Thacker, W. E. (1984). Simplified Models for Design of Fixed-bed Adsorption systems. Journal of Environmental Engineering, 110(2), 440-456.
13. Hlihor, R. M., & Gavrilescu, M. (2009). Removal of Some Environmentally Relevant Heavy Metals using Low-Cost Natural Sorbents. Environmental Engineering and Management Journal, 8(2), 353–372.
14. Hube, S., Eskafi, M., Hrafnkelsdóttir, K. F., Bjarnadóttir, B., Bjarnadóttir, M. Á., Axelsdóttir, S., & Wu, B. (2020). Direct membrane filtration for wastewater treatment and resource recovery: A review. Science of the Total Environment, 710.
15. Iftekhar, S., Ramasamy, D. L., Srivastava, V., Asif, M. B., & Sillanpää, M. (2018). Understanding the factors affecting the adsorption of Lanthanum using different adsorbents: A critical review. Chemosphere, 204, 413-430.
16. Ishak, A. R., Mohamad, S., Soo, T. K., & Hamid, F. S. (2016). Leachate and Surface Water Characterization and Heavy Metal Health Risk on Cockles in Kuala Selangor. Procedia - Social and Behavioral Sciences, 222, 263-271.
17. Jeyaseelan, C., & Gupta, A. (2016). Green Tea Leaves as a Natural Adsorbent for the Removal of Cr (VI) from Aqueous Solutions. Air, Soil and Water Research, 9, ASWR. S35227.
18. Khodami, S., Surif, M., Omar, W. M. W., & Daryanabard, R. (2017). Assessment of heavy metal pollution in surface sediments of the Bayan Lepas area, Penang, Malaysia. Marine Pollution Bulletin, 114, 615-622.
19. M., S., A.A., A., & M.T., A. (2018). Removal of Heavy Metals from Wastewater using Date Palm as a Biosorbent: A Comparative Review. Sains Malaysiana, 47(1), 35–49.
20. Mason, C. (2010). Lead and Pollution-an overview. Australian Journal of Public Health, 17(4), 296–298. https://doi.org/10.1111/j.1753-6405.1993.tb00156.x
21. Mondal, M. (2009). Removal of Pb(II) ions from aqueous solution using activated tea waste: Adsorption on a fixed-bed column. Journal of Environmental Management, 90 (11), 3266–3271.
22. Mondal, M. K. (2010). Removal of Pb(II) from aqueous solution by adsorption using activated tea waste. Korean Journal of Chemical Engineering, 27(1), 144–151.
23. Naiya, T. K., Bhattacharya, A. K., Mandal, S., & Das, S. K. (2009). The sorption of lead (II) ions on rice husk ash. Journal of Hazardous Materials, 163(2–3), 1254–1264.

24. Nikolic, M., Jeffry Robert, R., & Girish, C. (2019). The Adsorption of Cadmium, Nickel, Zinc, Copper and Lead from Wastewater using Tea Fiber Waste. Journal of Engineering and Applied Sciences, 14(20), 7743–7755.
25. Removal of Lead from Waste Water using Lantana Camara as Adsorbent. (2019). International Journal of Engineering and Advanced Technology, 8(6), 1531–1533.
26. Scala, F. (2001). Simulation of Mercury Capture by Activated Carbon Injection in Incinerator Flue Gas. 1. In-Duct Removal. Environmental Science & Technology, 35(21), 4367–4372.
27. Sulyman, M., Namiesnik, J., & Gierak, A. (2017). Low-cost Adsorbents Derived from Agricultural By-products/Wastes for Enhancing Contaminant Uptakes from Wastewater: A Review. Polish Journal of Environmental Studies, 26(2), 479–510.
28. Tee, T. W., & Khan, A. R. M. (1988). Removal of lead, cadmium and zinc by waste tea leaves. Environmental Technology Letters, 9(11), 1223–1232.
29. Wan, S., Ma, Z., Xue, Y., Ma, M., Xu, S., Qian, L., & Zhang, Q. (2014). Sorption of Lead(II), Cadmium(II), and Copper(II) Ions from Aqueous Solutions Using Tea Waste. Industrial & Engineering Chemistry Research, 53(9), 3629–3635.
30. Wang, J., Wang, T., Yan, B., Wang, Q., Zhang, Y., & Pan, W. P. (2021). Removal of ionic mercury from gasoline using zeolite 13X impregnated with KI: Adsorption mechanisms and simulation. Chemical Engineering Journal, 409, 128170.
31. Zhao, B., Zhang, Z., Jin, J., & Pan, W. P. (2009). Simulation of mercury capture by sorbent injection using a simplified model. Journal of Hazardous Materials, 170(2–3), 1179–1185.

London Journal Press Membership

For Authors, subscribers, Boards and organizations

London Journals Press membership is an elite community of scholars, researchers, scientists, professionals and institutions associated with all the major disciplines. London Journals Press memberships are for individuals, research institutions, and universities. Authors, subscribers, Editorial Board members, Advisory Board members, and organizations are all part of member network.

Read more and apply for membership here:
https://journalspress.com/journals/membership

For Authors

Author Membership provide access to scientific innovation, next generation tools, access to conferences/seminars /symposiums/webinars, networking opportunities, and privileged benefits.
Authors may submit research manuscript or paper without being an existing member of LJP. Once a non-member author submits a research paper he/she becomes a part of "Provisional Author Membership".

For Institutions

Society flourish when two institutions come together." Organizations, research institutes, and universities can join LJP Subscription membership or privileged "Fellow Membership" membership facilitating researchers to publish their work with us, become peer reviewers and join us on Advisory Board.

For Subscribers

Subscribe to distinguished STM (scientific, technical, and medical) publisher. Subscription membership is available for individuals universities and institutions (print & online). Subscribers can access journals from our libraries, published in different formats like Printed Hardcopy, Interactive PDFs, EPUBs, eBooks, indexable documents and the author managed dynamic live web page articles, LaTeX, PDFs etc.

GO GREEN AND HELP
SAVE THE ENVIRONMENT

JOURNAL AVAILABLE IN

PRINTED VERSION, INTERACTIVE PDFS, EPUBS, EBOOKS, INDEXABLE DOCUMENTS AND THE AUTHOR MANAGED DYNAMIC LIVE WEB PAGE ARTICLES, LATEX, PDFS, RESTRUCTURED TEXT, TEXTILE, HTML, DOCBOOK, MEDIAWIKI MARKUP, TWIKI MARKUP, OPML, EMACS ORG-MODE & OTHER

SCAN TO KNOW MORE

support@journalspress.com
www.journalspress.com

*THIS JOURNAL SUPPORT AUGMENTED REALITY APPS AND SOFTWARES